1978

# Ultrastructural studies of micro- and macrogametogenesis and oocyst wall formation in Eimeria nieschulzi a coccidian parasite of the rat

Gary Jay Sibert
*The University of Montana*

# ULTRASTRUCTURAL STUDIES OF MICRO- AND MACROGAMETOGENESIS AND OOCYST WALL FORMATION IN *EIMERIA NIESCHULZI*, A COCCIDIAN PARASITE OF THE RAT

by

Gary J. Sibert

B. A., University of Montana, 1976

Presented in partial fulfillment of the requirements
for the degree of

MASTER OF SCIENCE

UNIVERSITY OF MONTANA

1978

C A Speer
Chairman, Board of Examiners

R. C. Murray
Dean, Graduate School

10/30/78
Date





ProQuest LLC.
789 East Eisenhower Parkway
P.O. Box 1346
Ann Arbor, MI 48106 - 1346

Sibert, Gary J., MS August 1978 Microbiology

Ultrastructural Studies of Micro- and Macrogametogenesis and Oocyst Wall Formation in Eimeria nieschulzi, a Coccidian Parasite of the Rat. 75 pp.

Director: C. A. Speer CAS

The development of the endogenous sexual stages of Eimeria nieschulzi Dieben 1924 was studied with the electron microscope in experimentally infected juvenile rats.

Sexual stages, both micro- and macrogametocytes, developed from sexually indistinguishable 4th generation merozoites after a dedifferentiation process in which organelles of locomotion and penetration disappeared and organelles of synthesis and metabolism proliferated. There were also marked changes in the nucleus; from densely clumped peripheral chromatin in the merozoite to fine dispersed euchromatin in the late trophozoite.

Macrogametocytes were initially identified by the presence of dense type 2 wall forming bodies in the cisternae of rough endoplasmic reticulum. Amylopectin and lipid bodies appeared outside the cisternae of rough endoplasmic reticulum shortly before type 1 wall forming bodies appeared. Breakdown of wall forming bodies and subsequent oocyst wall formation were presumably initiated by fertilization. Unusual dense chromatinous nuclear inclusions were observed in zygotes during wall forming body breakdown and early oocyst wall deposition. Formation of both layers of the oocyst wall and proliferation of 7 membrane layers were observed. Oocysts with completed walls contained only small granular residua of wall forming bodies in the peripheral cytoplasm.

Trophozoites from dedifferentiated merozoites underwent nuclear division to produce microgametocytes. Mitosis occurred by intranuclear spindles without dissolution of the nuclear envelope. Neither discreet chromosomes nor actual separation of the dense chromatin was observed. Nuclear divisions initially occurred at the surface of the parasite. Surface invaginations occurred and carried some dividing nuclei to the interior where nuclear divisions continued. Centrioles involved with the mitotic spindle were always closely applied to the overlying surface membrane. After cessation of nuclear divisions, the chromatin condensed at the nuclear pole closest to the surface membrane. Flagella formed from centrioles (basal bodies) and protruded from the surface of the gametocyte. The condensed portion of each nucleus and a mitochondrion migrated into microgamete buds which contained a perforatorium and 2 flagellar apparati. Constriction by a dense ring containing microtubules beneath the surface membrane pinched-off the complete microgamete, freeing it into the parasitophorous vacuole.

Cytopathology induced by the sexual stages of E. nieschulzi in rat intestine is discussed.

ACKNOWLEDGMENTS

I would like to express my deepest appreciation to Dr. C. A. Speer for his assistance and guidance throughout this study.

I also wish to thank the other members of my degree committee: Drs. Card, Nakamura, Weisel, and Kilgore.

TABLE OF CONTENTS

LIST OF PLATES

## ABBREVIATIONS

### In Text

| | |
|---|---|
| EM | electron microscopy |
| m1 to m7 | parasite membranes numbered from periphery interiad |
| mv | membrane of the parasitophorous vacuole |
| nm | nanometer, $10^{-9}$ meter |
| PAS | periodic acid-Schiff staining procedure for polysaccharide |
| pv | parasitophorous vacuole |
| RER | rough endoplasmic reticulum |
| wf1 | wall forming body type 1 |
| wf2 | wall forming body type 2 |
| w/v | weight to volume |

### In Figures

| | |
|---|---|
| ap | amylopectin body |
| ar | apical rings |
| bb | basal body |
| bc | crescent body |
| ca | canaliculi |
| cb | condensation body |
| cc | centrocone of the mitotic spindle |
| ce | centriole |
| co | conoid |

| | |
|---|---|
| db | dense body associated with inner wall layer formation |
| dl | dense layer beneath membrane 7 |
| dr | dense ring |
| er | endoplasmic reticulum |
| f | flagellum |
| fs | fluid filled space in the oocyst |
| g | Golgi complex |
| if | intravacuolar folds |
| k | kinetochore (centromere) |
| lb | lipid body |
| ll | electron lucent layer |
| m | mitochondrion |
| m1 to m7 | parasite membranes numbered from periphery interiad |
| Mg | macrogametocyte |
| mg | microgametocyte |
| mi | inner membrane segment |
| mn | micromene |
| mp | micropore |
| MR | microgametocyte residuum |
| mt | microtubule |
| mv | membrane of the parasitophorous vacuole |
| n | nucleus of the parasite |
| nc | condensed nucleus of the microgamete |
| nd | nuclear detachment body |
| ne | nuclear envelope |

| | |
|---|---|
| nh | nucleus of the host cell |
| ni | nuclear inclusion |
| nr | nuclear residuum of the microgametocyte |
| nu | nucleolus |
| p | perforatorium |
| pv | parasitophorous vacuole |
| r | rhoptry |
| rbc | red blood cell |
| rf | rootlet of the flagellum |
| s | mitotic spindle |
| sm | subpellicular microtubule |
| st | spindle microtubule |
| v | microvillus |
| vm | vessicle associated with a micropore |
| wf1 | wall forming body type 1 |
| wf2 | wall forming body type 2 |
| wi | inner layer of the oocyst wall |
| wo | outer layer of the oocyst wall |
| Z | zygote |

# INTRODUCTION

## Taxonomic Classification of Eimeria nieschulzi Dieben 1924

Phylum PROTOZOA Goldfuss 1818, emend. Siebold 1845

Subphylum APICOMPLEXA Levine 1970

Class SPOROZOASIDE Leuckart 1879

Subclass COCCIDIASINA Leuckart 1879

Order EUCOCCIDIORIDA Leger and Duboscq 1910

Suborder EIMERIORINA Leger 1911

Family EIMERIIDAE Minchin 1903

Genus EIMERIA Schneider 1875

Species NIESCHULZI Dieben 1924

## History

The most recent review of history and taxonomy of the coccidia was given by Levine in 1973 (31). According to Levine (31), Eimeria stiedai from bile ducts in the rabbit was first seen by Leeuwenhoek in 1674, making it the first protozoan ever to be observed. However, coccidia were not described until 1839 when Hake considered E. stiedai to be a new type of pus globule from liver carcinoma in rabbits. Sporulation within the oocyst was first described in 1847 by Kauffman and the endogenous cycle was first described by Eimer in 1870. Eimer suggested the correct life cycle, which was vigorously contested. In 1892, alternation of generations was again postulated by L. Pfeiffer and R. Pfeiffer, but it was popularly held that the exogenous and endogenous stages were separate

genera; Coccidia Leuckart 1879, and Eimeria Schneider 1875, respectively.

Schuberg described the complete life cycle of Eimeria falciformis in 1897, proving the two stages to belong to the same organism. The genus Eimeria had priority so the term 'coccidia' has become a descriptive name for the entire group containing 34 genera in 10 families (31, 32).

The taxonomist Minchin in 1903 considered the entire sporozoa an obscure group of no practical importance. In 1906 Hartog wrote,

> "Coccidium may produce a sort of dysentery in cattle on alpine pastures of Switzerland; and cases of human coccidiosis are by no means unknown. Coccidium-like bodies have been demonstrated in the human disease 'molluscum contagiosum' and the 'oriental sore' of Asia; similar bodies have also been recorded in smallpox and vaccinia, malignant tumors, and even syphilis, but their nature is not certainly known; some of these are now referred to the flagellata." (32)

## General

Coccidiosis occurs in many wild and domestic animals and causes an annual loss of several million dollars to livestock and poultry producers in the United States alone (29). In areas of the world where food production in inadequate, such losses may be devastating. Coccidiosis may also be a threat to wildlife populations, especially in areas of high concentration and intensive management.

The signs of coccidiosis include diarrhea, weakness, and anorexia. Blood may or may not be present in the diarrheic feces. In severe cases, animals become emaciated, and death or retardation of growth occurs.

Coccidiosis is caused by protozoan parasites which belong to the genus Eimeria and related genera. Eimerian species are unusual among

parasites in their high degree of host specificity, infecting a single or a few closely related host species. Certain other genera of coccidia are very host specific, whereas others have a wide host range. Most of the animal species which might harbor coccidia have not yet been examined for these parasites. By 1962, only 539 species of Eimeria had been described, representing as estimated 1.5% of the total number present in chordates alone (29). Pellérdy in 1974 listed 973 species of Eimeria that occur in animals from annelids to mammals (41). Coccidian species are differentiated on the basis of structural and biological characteristics. Since the endogenous stages in the life cycle of most species are unknown, the structure of the sporulated oocyst is the most commonly used taxonomic parameter. The opinion is sometimes expressed that oocysts contain so few structures that not many species can be distinguished on that limited basis, but conservative calculation indicates that at least 2,654,736 structurally different oocysts are possible in the genus Eimeria alone (30).

The typical eimerian life cycle includes endogenous stages, occurring within the host, and exogenous stages outside the host. Outside the host and in the presence of oxygen, the oocyst protoplasm or sporont undergoes a series of divisions referred to as sporogony, which results in the formation of four sporocysts, each with two sporozoites. Sporulated oocysts are infective to another susceptible host. After the oocyst has been ingested by a suitable host, carbon dioxide, trypsin, and bile salts in the intestine cause sporozoites to actively escape from the sporocyst and then the oocyst. Sporozoites penetrate intestinal epithelial cells and undergo asexual reproduction

to produce several to several thousand merozoites. Merozoites invade adjacent cells or escape into the lumen and move down the intestine before invading other epithelial cells. There may be one to several such asexual generations. Merozoites of the last asexual generation develop into female macrogametocytes or male microgametocytes. The macrogametocyte produces only a single nonmotile gamete, whereas the microgametocyte produces many flagellated microgametes. Soon after fertilization, the zygote forms a highly resistant peripherally located wall complex and presumably releases toxins which cause death and sloughing of the host cell. With completion of the resistant wall, the parasite is called an oocyst and is passed in the feces (16, 41).

Fine structural aspects of macrogametogenesis have been studied in several species of Eimeria (6, 7, 12, 21, 27, 37, 45, 46, 48, 49, 50, 51, 52, 54, 55, 56, 57, 60, 64, 66, 70); however, many problems remain unresolved. For instance, little is known about the mechanism of oocyst wall formation, which presumably begins shortly after fertilization of the macrogamete by the microgamete. Studies on formed walls (39, 42, 43, 54, 57, 62, Speer unpublished) have been able to only suggest modes of formation. Microgametogenesis and nuclear division have also been studied in several eimerian species with the electron microscope (4, 5, 7, 9, 10, 11, 13, 18, 20, 22, 24, 26, 35, 36, 45, 46, 47, 53, 59, 61, 68). Hammond and Scholtyseck found microgametes within the macrogamete cytoplasm (19, 49), but penetration by the microgamete and fusion of the micro- and macrogamete nuclei have not yet been recorded.

Several studies of sporulation have been made with light microscopy (16, 71), but little information has been obtained by electron microscopy. Birch-Andersen, et al. (1) published a method of obtaining thin sections of sporulated oocysts for electron microscopy from frozen thick sections. Using that procedure, Ferguson et al. (13) have published electron micrographs of the sporoblast stage of Eimeria brunetti, but the quality of the micrographs produced is less than desired.

## Cytochemistry

Identification of subcellular structures by cytochemical means was reviewed by Ryley (43). Large pale to clear bodies in macrogametocytes under the light microscope were described by Cross (8) as lipid by use of Sudan 4 staining and again by Pattillo and Becker (40) using Sudan Black B. Such bodies are easily identified in electron microscopy by position in the cell, size, and electron density.

The periodic acid-Schiff (PAS) technique was first applied to coccidian macrogametocytes by Gill and Ray (14), confirming the presence of a polysaccharide then believed to be glycogen due to its destruction by amylase. Actually, the PAS reaction is given by any polysaccharide complex containing adjacent diol groups (-CHOH·CHOH-). This includes glycogen, amylose, amylopectin, dextran, 1,4-xylan, and cellulose. The amylase control eliminates dextran, xylan, and cellulose due to the lack of $\alpha$-1,4-glucosidic linkages attacked by the enzyme. Extraction of polysaccharide from endogenous stages of E. tenella and E. brunetti with hot 20% KOH and subsequent biochemical

characterization by Ryley et al. (44) indicated an α-1,4 linked glucosyl chain containing α-1,6-glucosidic branch points, eliminating amylose. By differences in physical characteristics such as solubility, viscosity, and the interaction with iodine, the polysaccharide was determined to be amylopectin due to its longer chain lengths and resulting more open structure than glycogen. A modification of the PAS technique, substituting thiocarbohydrazide silver-protein for the Schiff reagent was first used by Thièry (65) for electron microscopy to positively identify electron transparent bodies in marcogametocytes as polysaccharide, and therefore as amylopectin.

Pattillo and Becker (40) characterized the 'plastic granules' or wall forming bodies in macrogametocytes and the oocyst wall as protein by specific staining for light microscopy with mercuric bromphenol blue.

Due to the oocyst wall, oocysts are extremely resistant to conventional disinfectants such as potassium dichromate ($K_2Cr_2O_7$), concentrated sulfuric acid ($H_2SO_4$), or sodium hypochlorite (NaOCl) (43). Sterilization can be accomplished with high concentrations of small molecular substances such as ammonia, methyl bromide, and carbon disulfide (43).

By light microscopy, Henry (23) and Cheissin (2) determined that oocyst walls had two or sometimes three layers. The outer layer was thought to be fairly rigid and chitinous or keratinous, whereas the inner layer was more elastic, responding to osmotic conditions. Grasse (15) and Cheissin (3) proposed that the two distinct wall layers form from two separate types of 'plastic granules' or wall forming bodies. Polarized light microscopy of the oocyst wall by Monné and Hönig (38) showed the outer layer to be weakly birefringent

or isotropic, whereas the inner layer had different refringence patterns for the inner and outer surfaces. The inner portion of the inner layer was positively birefringent and scattered light, indicating lipid. The outer portion of the inner layer was negatively birefringent in a radial direction, indicating protein. The outer layer could not be dissolved in concentrated sulfuric acid, sodium sulfide, or thioglycollate, ruling out chitin (38). Wilson and Fairbairn (71) found that the outer layer was not susceptible to chitinase, indicating no N-acetyl glucosamine. The outer wall layer was determined to be composed of a quinone-tanned protein on the basis of its solubility in sodium hypochlorite (NaOCl) and its ability to reduce ammoniacal silver nitrate (38).

Ryley (43) reported that the outer wall layer comprised 19.5 to 21.8% of the total dry weight of the oocyst. He also reported preliminary chemical analysis of the inner layer but cautioned that isolation of samples uncontaminated with inorganic material was extremely difficult. The inner layer was roughly 70% protein with a high proline content and no basic amino acids, 30% lipid containing a mixture of waxes with chain lengths of up to 40 carbons, and about 1.5% carbohydrate (43). Location of protein within the layers was tested by susceptibility to three proteolytic enzymes; pepsin, pronase, and trypsin. Three configurations were tested; (i) intact oocysts with an intact outer layer, (ii) oocysts stripped of the outer layer with NaOCl which exposed the exterior surface of the inner layer, and (iii) mechanically fractured inner layer fragments. Enzyme efficacy was expressed as the percent amino nitrogen solubilized. Solubilization of

intact oocysts was less than 0.5%, stripped oocysts less than 10%, and fractured oocyst walls greater than 90%, indicating that an outer limiting membrane may protect the outer layer and a waxy layer protects the intact inner layer (43).

Early electron microscopic studies by Scholtyseck and Voigt (54) confirmed the postulate of Grasse (15) and Cheissin (3) that separate types of wall forming bodies gave rise to the separate wall layers. Both types of bodies seen with the electron microscope stain intensely with mercuric bromphenol blue under the light microscope, indicating protein (38). Treatment with weak NaOCl destroys mercuric bromphenol blue staining ability of type 1 wall forming bodies (wf1) but not of the type 2 (wf2). It was also found that wf1 show weak staining with periodic acid-Schiff (PAS) which is not affected by amylase pretreatment, indicating some glycoprotein content (38). Type 2 wall forming bodies were PAS negative (38). EM studies of isolated fractured oocyst walls (39, 42, 43, 62, Speer unpublished) do not show the separation of protein and lipid in the inner wall layer into distinct strata as suggested by polarized light microscopy (38), indicating a structure of protein matrix impregnated with lipid.

## Eimeria nieschulzi

Eimeria nieschulzi is a coccidian parasite with a strict host specificity for rats (Rattus rattus, Rattus norvegicus, and Rattus hawaiiensis) and which causes a severe, often fatal dysentery in young rats characterized by a catarrhal hemorrhagic enteritis of the small intestine. It was first described as a species in 1924 by C. P. A.

Dieben in his dissertation , "Over de Morphologie en Biologie van het Ratten-coccidium Eimeria nieschulzi n. sp. en zijne Verspreiding in Nederland" (41). Since this time, E. nieschulzi has become a commonly used species for investigation of physiology and immunity because it is relatively easily maintained in the laboratory.

Both the endogenous and exogenous stages of E. nieschulzi have been studied by light microscopy (33, 41). Colley (7) reported brief ultrastructural studies of the endogenous stages. However, these studies were incomplete and based upon information obtained from relatively poor electron micrographs. Due to recent improvements in preparing coccidian parasites for electron microscopy, much more fine structural detail can now be obtained.

According to Pellérdy (41), oocysts of E. nieschulzi are passed in the rat feces and undergo sporogony in the presence of oxygen in 65 to 72 hours, during which meiosis presumably occurs. The sporont divides to form sporoblasts which in turn form four sporocysts, each containing two sporozoites. Upon ingestion of oocysts by a susceptible rat, sporozoites escape from the sporocyst and then the oocyst and appear free in the intestinal lumen at four hours. Sporozoites invade intestinal epithelial cells where there are four asexual schizont generations. First generation schizonts appear at 31 to 36 hours, each producing 20 to 36 merozoites; the second generation occurs at about 48 hours with 10 to 14 merozoites; the third generation at about 72 hours with 8 to 20 merozoites; and the fourth generation at about 96 hours with 36 to 60 merozoites, which then develop into gametocytes. Thus, each sporulated oocyst ingested has the potential of producing

over 4.8 million gametocytes, of which at least half are female and capable of developing into infective sporulated oocysts. Gametogenesis commences at about 100 hours and oocysts first appear in the feces at 7 to 8 days. If the host survives, the infection is generally cleared by day 10 and a fairly solid species-specific immunity results (41).

It was the purpose of this study to characterize the ultrastructural changes accompanying gametogenesis and oocyst wall formation in Eimeria nieschulzi Dieben 1924.

# MATERIALS AND METHODS

## Animals

A colony of outbred albino rats (Rattus norvegicus), obtained from the Zoology Department of the University of Montana, was maintained in stainless steel cages with wire mesh floors. Purina Lab Chow and water were fed ad lib.

## Parasites

A stock of Eimeria nieschulzi oocysts was obtained from the University of New Mexico Department of Zoology in 1976 and stored at 4°C in 2.5% potassium dichromate ($K_2Cr_2O_7$). Serial passages through rats were made at various intervals to maintain a fresh stock of oocysts. Fresh fecal pellets containing unsporulated oocysts were collected in 2.5% $K_2Cr_2O_7$, shaken vigorously to disrupt pellets, and swirled 72 hours on a magnetic stirrer to induce sporulation. The stirring mixture was kept in a water bath at room temperature to dissipate heat buildup. The slurry containing sporulated oocysts, fecal matter, and $K_2Cr_2O_7$ was washed through 20 and 50 mesh sieves, then sedimented by centrifugation (450 X g), resuspended in distilled water, and resedimented four times to remove the $K_2Cr_2O_7$. Oocysts were concentrated by digesting the pellet in 2.5% sodium hypochlorite (NaOCl) for 30 minutes at 0°C to remove fecal organic matter and sterilize the oocyst surface (69). This treatment may also facilitate excystation since the outer layer of the oocyst wall is removed (43). Oocysts were separated from residual fecal material by floatation on

20% (w/v) sodium chloride (NaCl), collected by aspiration, and washed repeatedly in distilled water by centrifugation (450 X g). Suspensions were quantified by counting sporulated oocysts on a hemacytometer.

## Infection of Animals

Juvenile rats from 1 to 2 months old were anesthetized with ether and inoculated by gavage with $10^5$ to $10^6$ sporulated oocysts of Eimeria nieschulzi in distilled water. Polyethylene intravenous tubing 0.034 ID by 0.050 OD by 15 cm long attached to a 1.0 ml syringe with a 22 gauge needle was used as the gavage apparatus.

## Collection of Tissues

At 12 hour intervals from 96 to 180 hours after inoculation, animals were anesthetized with ether and intestinal tissues were surgically removed. Tissue samples were minced to 0.5 mm cubes in fixative and transferred to vials containing fresh fixative at about 21°C.

## Fixation

The best fixation was obtained with 3% glutaraldehyde in 0.2 M cacodylate buffer, pH 7.25 for 3 hours at 21°C. After overnight rinses in cold cacodylate buffer, specimens were post-fixed in cold osmium tetroxide ($OsO_4$) in cacodylate buffer for 2 hours.

## Preparation of Tissues for EM

After post-fixation in $OsO_4$, tissues were washed in cold buffer

and partially dehydrated through a graded ethanol series at 10 minute intervals. En bloc staining was carried out in 1% (w/v) phosphotungstic acid and 1% (w/v) uranyl acetate in 70% ethanol for 18 hours at 4°C. Tissues were dehydrated completely by 10 minutes intervals in 95% and 100% ethanol and 2 changes of propylene oxide. Infiltration with epoxy resin, either Epon 812 or Spurr's low viscosity embedding medium, was carried out stepwise in 1:1 epoxy to propylene oxide for 1 hour, 3:1 epoxy to propylene oxide for 18 hours, and pure epoxy for 12 hours. Tissue specimens were continuously agitated during infiltration with a Pelco Infiltron rotator. Tissue blocks were placed in molds with fresh resin and polymerized at 60°C for 20 to 30 hours.

Ultrathin sections, 6 to 12 nm in thickness, were cut on glass or diamond knives with a Porter-Blum MT-2 ultramicrotome, placed on uncoated 200 or 300 mesh copper grids, and stained 5 to 10 minutes with lead citrate. All observations were made with a Zeiss EM9-S2 electron microscope.

Semithick sections of 0.5 to 1.5 µm were cut from epoxy tissue blocks, heat fixed to glass slides, and stained with Paragon epoxy tissue stain for light microscopy to determine heavily infected areas for examination by electron microscopy.

Over 2,000 specimens were observed and 650 electron micrographs were made in the course of this study.

# RESULTS

## Trophozoites

It was not possible to differentiate macrogametocytes from microgametocytes until certain organelles appeared in the former and nuclear division commenced in the latter. Therefore, all undifferentiated uninucleate parasites are herein referred to as trophozoites.

The sexual phase of the life cycle of Eimeria nieschulzi commences at the end of the fouth merogonous generation in epithelial cells of the rat intestine. The fourth generation merozoite (Fig. 1) enters a new host cell and develops into a micro- or macrogametocyte. Soon after entering a host cell, the merozoite underwent a process of dedifferentiation in which it was transformed from a vermiform to a spheroidal shape. During this process, many of the organelles peculiar to invasive stages disappeared, including apical rings, conoid, polar rings, rhoptries, micronemes, subpellicular microtubules and an inner membrane complex of two closely applied unit membranes. The merozoite nucleus had coarse peripheral heterochromatin, coarse nucleoplasm, and a very diffuse nucleolus, whereas the late trophozoite nucleus had fine granular euchromatin and a large spheroidal nucleolus (Fig. 2-4). Apical complexes (i.e. conoid, polar rings, and rhoptries) were observed only in merozoites budding from schizonts, and not in single specimens within epithelial cells, indicating early degeneration of these organelles after penetration of the host cell. Subpellicular microtubules also disappeared during transformation to the spheroidal shape (Fig. 3). Micronemes and portions of the inner membrane complex

appeared to be retained longer than any other organelles peculiar to merozoites. With the disappearance of the organelles associated with merozoite motility and penetration, there was a proliferation of organelles of metabolism and secretion such as mitochondria, endoplasmic reticulum, and Golgi complexes. Trophozoite mitochondria were greatly enlarged compared to the mitochondria of infected intestinal cells, which were larger than those of adjacent uninfected cells (Fig. 3).

After an initial enlargement, trophozoite mitochondria apparently underwent division which ultimately produced several smaller mitochondria. Golgi complexes also increased in number with one such complex being intimately associated with a ribosome-free area of the nuclear envelope, while others were more peripherally located and closely associated with endoplasmic reticulum (Fig. 5). Moderately electron dense bodies averaging 200 nm in diameter with electron dense cores were associated with Golgi complexes (Figs. 5, 6, 10, 11). Such bodies were not membrane bound and occurred in both developing macrogametes and early multinucleate microgametocytes and therefore were not considered to be involved in oocyst wall formation. Also seen in most specimens were several eclipse-like condensation bodies with an extremely electron dense spherical core averaging 95 nm in diameter, an electron dense peripheral sphere averaging 210 nm in diameter, and an electron transparent inner space (Fig. 9). Similar bodies were also observed in intestinal spirochetes, but never within host tissues.

## Early Macrogametocytes

Early macrogametocytes were identified by the presence of spherical homogeneous electron dense type 2 wall forming bodies (wf2) in the cisternae of the peripheral rough endoplasmic reticulum (RER) (Figs. 6, 8, 10, 11). In such specimens the RER was extensive and contained a moderately electron dense homogeneous material. Dense cored bodies described above were free in the cytoplasm. The single limiting membrane (ml) or plasmalemma contained typical micropores (Figs. 6, 7) and in some specimens was in direct contact with intravacuolar folds of the parasitophorous vacuole membrane (mv) (Figs. 8, 10, 11, 12, 14). Occasionally in early macrogametocytes, active micropores contained granular material similar to that present in the parasitophorous vacuole (Fig. 7). However, most micropores observed in early macrogametocytes, as well as later stages, were inactive. Nearly all young macrogametocytes had segments of a double membrane complex immediately beneath the plasmalemma. Such membrane fragments may represent remnants of the inner membrane complex of the merozoite or newly synthesized membrane. Some early macrogametocytes also had double membrane bound granular bodies of low electron density similar to those described by other authors as nuclear detachment bodies (70), but which differed markedly from nucleoplasm in E. nieschulzi. One such specimen had a centriole associated with a thickening of both membranes of the nuclear envelope (Fig. 8). Some specimens had a well segregated mass of dense clumped chromatin at one side of the nucleus (Figs. 6, 8).

## Intermediate Macrogametocytes

Intermediate stages of macrogametogenesis were characterized by an increase in size and by the appearance of rod-shaped electron transparent amylopectin bodies about 100 nm by 300-400 nm in size and closely associated with the ribosomal surface of the RER and the outer nuclear membrane (Figs. 10, 11). Few or no lipid bodies were present when amylopectin first appeared, but lipid bodies became evident when amylopectin bodies were enlarged. Type 2 wall forming bodies (wf2) were larger and more numerous than in early macrogametocytes. Dense cored bodies were free in the cytoplasm and appeared enlarged and less dense in some specimens. The nucleus closely resembled that of the early macrogametocyte except that the area of coarse chromatin was no longer evident. The intermediate stage appears to be very transitory, since only a few specimens were observed.

## Mature Macrogametes and Zygotes

The mature stages of macrogametogenesis were considered those specimens with type 1 wall forming bodies (wf1) present in the cytoplasm. Wf1 were membrane bound, free in the cytoplasm, were extremely electron dense prior to fertilization, and generally lay peripheral to type 2 wall forming bodies (wf2). Wf1 apparently arose within the cytoplasmic ground matrix and reached a maximum diameter of about 0.94 um. Wf2 in mature gametes measured up to 1.06 um, were finely granular with a lesser electron density than wf1, and lay within cisternae of RER. Mature macrogametes had relatively large spheroidal or ellipsoidal amylopectin bodies which measured up to 900 nm in

diameter. Canaliculi, the so-called 'canal system of the endoplasmic reticulum' (48), contained a homogeneous nongranular material of low electron density similar in appearance to lipid bodies. Canaliculi and lipid bodies were located between the nucleus and the peripherally situated wall forming bodies (Figs. 12, 14). The innermost membrane (m2) lay immediately beneath the limiting membrane of the intermediate macrogametocyte (ml). Peripheral mitochondria were densely granular or appeared vestigial. A single mitochondrion was seen in close association with the nucleus in some sections (Fig. 21). Golgi complexes were reduced or absent.

The nucleolus was more condensed and spherical, and the nucleoplasm was more homogeneous with fine granular euchromatin that in early or intermediate macrogametocytes. Several specimens at this stage, as well as those in which oocyst wall formation had begun, had a second electron dense body within the nuclear envelope. The nuclear inclusion was chromatinous rather than nucleolar in appearance (Figs. 12, 13). At present, its significance is not known, but it may represent a microgamete nucleus after fertilization. Although microgametes were seen occasionally in cells adjacent to macrogametocytes (Figs. 21, 50), neither microgametes in the parasitophorous vacuole of a macrogametocyte nor fertilization were observed.

## Oocyst Wall Formation

Initiation of oocyst wall formation was first indicated by the appearance of curved or circular patterns of granularity within wfl (Figs. 14, 15). Such patterns suggest that an enzyme was added at

the margin and penetrated into the wf1. Following granulation, the wf1 were reduced to small electron dense bodies about 150 nm in diameter which were separated from the cytoplasmic ground matrix by a thin halo (Fig. 17). Such reduction presumably occurred by transport of granules away from the wf1 into the cytoplasm, but the density of the surrounding cytoplasm obscurred visualization of the process.

After breakdown of wf1 and before deposition of the outer layer of the oocyst wall, small granules, 40 to 50 nm in diameter, appeared at the margins of wf2 (Figs. 16, 17). During the formation of such granules, the inner regions of the wf2 became honeycombed or labyrinthine in appearance (Figs. 16-19).

During oocyst wall formation, extensive membrane proliferation occurred at the surface of the parasite. Two surface membranes were present when breakdown of wf1 began, three when wf2 breakdown began, and four at the time of outer wall layer deposition (Figs. 18-22). The original trophozoite membrane (m1) was located at some distance from the body of the zygote and in some areas was in contact with the intravacuolar folds of the vacuolar membrane (Figs. 16-22). Membrane 2 was the outer limit of the forming outer layer of the oocyst wall. Membrane 3 occurred in segments and formed the inner limit of the outer wall layer. Membrane 4 was immediately beneath membrane 3 and the innermost surface membrane of the parasite when deposition of the outer wall layer began (Figs. 19, 22).

The outer layer of the oocyst wall formed first and initially appeared as fine granular material similar to that formed earlier by granulation of wf1. In some specimens, dense concentrations of

granules from wf2 breakdown underlay areas of apposition between segments of m3 (Fig. 19). After transport across m4, this material was apparently transported through the gaps or across intact areas of m3, since 40 to 50 nm particles similar in appearance to wf2 granules accumulated with fine granular material between m2 and m3 (Figs. 19, 20, 22). No evidence of exocytosis or fusion of membrane bound bodies with a surface membrane was observed.

Two distinct patterns were observed in the disintegration of wf2 and formation of the outer wall layer, even among specimens from the same tissue block. In pattern A, the wall forming material lying between m2 and m3 remained in a loose granular configuration after deposition until the inner wall layer was nearly complete. Wf2 in specimens displaying pattern A were labyrinthine (Figs. 18, 19, 26, 27). In pattern B, granules between m2 and m3 coalesced into a relatively homogeneous and finely granular electron dense layer before deposition of the material was complete. Wf2 in pattern B specimens were more homogeneous and electron dense than in pattern A (Figs. 20-22, 30). Associated with both patterns of outer wall layer deposition was an increase in the number of lipid bodies and a slight shrinking of the amylopectin bodies, most of which were closely associated with lipid bodies (Figs. 16, 18, 21). Also in both patterns, vacuoles surrounding adjacent wf2 appeared to fuse to form larger vacuoles (Figs. 20, 21). Some specimens had incomplete outer wall layers when inner layer deposition began (Figs. 23, 24), suggesting that a flowing of the outer layer over the surface might occur in order to form a complete outer wall layer. Several specimens had extensive folding

and overlapping of membranes 1 through 4 (Figs. 23-25), which also suggests that there be a flowing of membranes over the surface of the organism.

Before deposition of the inner layer of the oocyst wall, membranes 5 and 6 appeared beneath m4 (Fig. 24). Before the coalescence of the material forming the inner layer, m7 appeared immediately beneath m6 (Figs. 26, 27). Several layers of RER were located close to the surface of the parasite and may have given rise to the new inner surface membranes (Figs. 24, 25).

Two patterns of inner wall deposition were observed. In pattern C, finely granular material of low electron density was transported or exocytosed into a space between m4 and m5 (Figs. 23-25). Relatively large electron dense spherical bodies which appeared to have been exocytosed intact were also present between m4 and m5 (Fig. 24). Some of these bodies assumed a flattened shape immediately beneath m5 (Fig. 25). The peripheral cytoplasm contained amorphous areas bounded by RER that had an electron density similar to that of the inner wall material (Figs. 23, 24). Figure 24 suggests that such material entered the space between m4 and m5 by exocytosis. In some areas, small globules of wall forming material occupied a space immediately beneath m6 (Fig. 24). Membrane 7 had attached ribosomes, indicating that it was peripherally located RER (Figs. 25, 26). During condensation of the outer wall layer, the electron density most closely resembling the fully formed layer occurred next to m3, whereas the outer portion was less electron dense (Fig. 23). This suggests that condensation of the outer layer progressed outward from membrane complex m3-m4.

Pattern D inner layer formation (Figs. 26, 27) occurred in those specimens displaying pattern A outer layer formation. In such specimens, the outer layer of the oocyst wall was still granular when moderately electron dense spheroidal bodies between m4 and m5 began to coalesce into irregularly shaped globules which ultimately coalesced completely to form a continuous inner wall. Membrane 7 limited the cytoplasm and in one specimen appeared to be in close association with a canaliculus (Fig. 26). Immediately beneath m7 in some specimens, there was a highly electron dense layer, apparently formed by the coalescence of flattened electron dense bodies (Figs. 27, 28). In one specimen, the electron dense layer extended into the cytoplasm of the zygote forming a loop (Fig. 27).

Before completion of both layers of the oocyst wall, the cytoplasm of the late zygote contained numerous lipid and amylopectin bodies, large labyrinthine wf2 with a finely granular matrix, small haloed bodies of high and moderate electron density, rough endoplasmic reticulum, extremely dense free ribosomes, canaliculi, and membranous granule-filled structures suggestive of degenerate mitochondria (Figs. 26, 27).

## Oocysts

Upon completion of the double layered peripheral wall complex, the parasite became an oocyst. Due to the extreme resistance of this stage to infiltration by fixatives and embedding resins, only a few specimens were available for study. In some specimens, the inner and outer layers of the oocyst wall separated, creating a space (Fig. 28). Evidently, the inner wall layer is more resistant to fixatives and embedding resins

than the outer layer since only a few intact specimens were obtained after formation of the inner wall layer. The separation of the wall layers may be due to osmotic differentials caused by low permiability of the inner layer as reported by Cheissin (2).

As in the late macrogamete and zygote, the nucleus contained euchromatin and a compact spherical nucleolus (Fig. 28). Due to the fragility of incompletely fixed and embedded specimens, serial sections of the entire nucleus were not available to determine the presence or absence of the dense nuclear inclusion body. The cytoplasm contained canaliculi and was nearly completely filled with lipid and amylopectin bodies in a dense matrix of ribosomes. The peripheral cytoplasm contained numerous spheroidal bodies of moderate electron density (Figs. 28, 29).

Soon after the oocyst wall was completely formed, the protoplasm or sporont condensed, pulling away from the inner surface of the oocyst wall, creating a fluid-filled space which contained a network of granular material between the sporont and the oocyst wall (Figs. 29, 31). The complete oocyst wall had a finely granular, moderately electron dense inner layer with a uniform thickness of 150 to 220 nm; a uniform electron lucent layer consisting of membranes m3-m4 interposed between the inner and outer layers; and an extremely electron dense, finely granular outer layer that varied in thickness from about 50 to 300 nm with the thinnest portion located at the micropylar pole.

## Microgametogenesis

As stated earlier, it was not possible to determine which tropho-

zoites would develop into macro- and microgametocytes. It was also very difficult to differentiate early multinucleate microgametocytes from early schizonts. In order to obtain tissues with a maximum number of microgametocytes and a minimum number of schizonts, infected tissues were taken between 144 and 168 hours after inoculation. Such tissues contained more mature microgametocytes than earlier tissues since microgametogenesis appeared to progress slightly slower than macrogametogenesis.

## Nuclear Division

Nuclear division in a late trophozoite was the earliest indication of microgametogenesis (Fig. 32). In the first nuclear division, the nucleus and nucleolus both became elongate with the latter becoming diffusely rod shaped. Two distinct areas of coarsely granular heterochromatin in the finely granular nucleoplasm were located lateral to the nucleolus near the opposite poles of the nucleus. The cytoplasm contained those inclusions described above for trophozoites. The plasmalemma was closely associated with the parasitophorous vacuolar membrane (Fig. 32), whereas in multinucleate forms, a prominant parasitophorous vacuole (pv) surrounded the parasite (Fig. 35). Occasionally, a typical crescent body was present within the pv. Shortly after the first nuclear division, there was a rapid proliferation of rough endoplasmic reticulum, Golgi complexes, and mitochondria (Figs. 33, 35). Most mitochondria were situated immediately beneath the plasmalemma; some at areas of contact between ml and mv (Figs. 32, 33, 35). Binucleate and multinucleate stages

contained nuclei in which most of the chromatin was clumped at the nuclear membrane. With an increase in the number of nuclei, there was a progressive decrease in the size of the nucleolus until it ultimately disappeared (Figs. 33-41). Nuclei in different stages of division were seen in the same parasite, indicating that nuclear division was asynchronous (Figs. 33-40). Mitotic apparati were observed in most multinucleate specimens (Figs. 33-40). Each dividing nucleus had 2 pairs of centrioles closely associated with the nuclear envelope. Initially, the two pairs of centrioles lay in close proximity between the nuclear envelope and the plasmalemma (Fig. 39). Later, as the nucleus elongated, each centriolar pair migrated to opposite poles of the nucleus. A centrocone and spindle apparatus formed at each pole of the nucleus and division occurred acentrically (Figs. 33-38, 40). The open end of each centriole was oriented away from the centrocone and was in close proximity to the plasmalemma. Asters of microtubules were never observed around centrioles either when the spindle was present (Fig. 34) or between nuclear divisions (Fig. 39). During nuclear division, the nuclear envelope remained intact with the spindle occurring within the nucleus (Figs. 34-40). The microtubules of the centrocone appeared to traverse the nuclear envelope (Figs. 34, 38, 40). Two types of spindle microtubules were present: (i) short microtubules which extended from the centrocone to kinetochores (centromeres) on loosely coiled chromosomes in the chromatin aggregation resembling a metaphase plate (Fig. 36), and (ii) longer microtubules extending across the central region of the chromatin plate (Fig. 37).

The gametocyte increased in size from about 4.5 μm in diameter at

the first nuclear division to about 12 μm in diameter as a mature multinucleate microgametocyte. Early and intermediate nuclear divisions occurred at the periphery of the cell (Figs. 35, 38). In the latter stages of nuclear proliferation the gametocyte plasmalemma underwent extensive invagination which increased the surface area many times (Fig. 40). After invagination, nuclear divisions continued with each nucleus and its centrioles closely associated with the plasmalemma. The first indication of microgamete formation was marked by the appearance of an electron dense membrane segment beneath the plasmalemma and immediately above each nucleus and centriolar pair (Fig. 40). Mitochondria in early stages were randomly distributed throughout the gametocyte, whereas in intermediate stages, most mitochondria were closely associated with nuclei (Figs. 41, 43).

## Intermediate Microgametocytes

After nuclear divisions ceased, condensation of dense chromatin occurred toward the associated surface membrane of each nucleus (Figs. 41, 42). Simultaneously with the process of nuclear condensation, microgamete flagella were formed by protrusion from the surface of the gametocyte above centrioles (Figs. 41, 42). Microgamete flagella were typical of certain eukaryotic cells in that they consisted of microtubules arranged in a configuration of nine peripheral pairs and two unpaired central microtubules (Figs. 42, 47). Each flagellum arose from a basal body (centriole) containing nine peripheral triplets arranged in a cylindrical structure and a single short central microtubule only at the proximal (closed) end (Figs. 39, 42). Each basal

body was connected to its perpendicularly oriented sister basal body by an electron dense, helical rootlet (Figs. 42, 49).

The anterior tip of the developing microgamete contained the perforatorium, two basal bodies, flagellar rootlets, and two flagella, and was completely developed before the nucleus was fully condensed. The condensed portion of the nucleus and the mitochondria lay within the microgamete bud which was connected to the gametocyte by a stalk consisting of uncondensed nucleoplasm, the nuclear envelope, the dense ring, and the plasmalemma. The dense ring, corresponding to the electron dense membrane segment described above, contained two circular microtubules at the outer end and lay immediately beneath the plasmalemma in the stalk (Figs. 44, 48). When nuclear condensation was complete, the dense ring was constricted and the microgamete was pinched off, leaving moderately electron dense nucleoplasm in the nuclear residuum within the gametocyte (Figs. 44, 46, 48).

## Mature Microgametes

The microgamete body was covered by a single membrane with a uniform amorphous 7 nm coating and contained a highly electron dense granular nucleus with a single nuclear membrane, a single mitochondrion, three or more microtubules, two basal bodies with rootlets of two flagella, and an electron dense plate-like perforatorium (Figs. 44-46, 49). The perforatorium was granular, formed an apex at the anterior tip, and extended posteriorly beneath the surface opposite the mitochondrion to a point just anterior to the nucleus where it terminated in a bulbous structure (Figs. 46, 49).

After complete microgametes were pinched off into the parasitophorous vacuole, the microgametocyte residuum condensed to a roughly spherical body containing mitochordria, residual nucleoplasm, amylopectin deposits, and dense rings and micropores along the surface. All internal architecture degenerated rapidly (Fig. 48). One section through a microgametocyte residuum showed 54 microgametes cut through the body within the parasitophorous vacuole (Fig. 48). The parasitophorous vacuole was about 15.4 μm and the microgametocyte residuum was about 7.5 μm in diameter. Assuming both to be roughly spherical, the volume of the parasitophorous vacuole not occupied by the residuum was about 1700 $\mu m^3$. Since the longest portion of a microgamete body observed was about 2.5 μm, that was taken as the thickness of the section, so the volume containing 54 gametes was considered to be 350 $\mu m^3$. Then, by conservative estimate, it is possible that $54 \times \frac{1700}{350} =$ 260 microgametes were produced from a single gametocyte.

## Host Cell Pathology

Pathological changes in host cells were evident early in the development of the parasite as well as in later stages (Figs. 4, 12, 30, 41, 43, 48, 49, 50). Microvilli of the brush border were much reduced and the substructure of the terminal web was disorganized (Figs. 30, 33). The host cell nucleus often had a distorted surface and was displaced toward the lumen (Figs. 4, 12, 30, 41, 43). Host cell mitochondria were often closely associated with the vacuolar membrane (Figs. 3, 4). A disruption of the cytoplasmic matrix observed in one host cell containing a trophozoite may correspond to the path

of the invading merozoite (Fig. 4).

Migration by microgametes caused considerable cytopathology. A nucleus penetrated by a microgamete was quite pyknotic compared to adjacent cell nuclei (Fig. 50). There was extensive degeneration of cytoplasmic architecture in the host cell before migration and a foamy appearance to the host cell and neighboring cell cytoplasm after migration (Figs. 48-50).

Oocysts were released into the lumen by death of the host cell.

## EXPLANATION OF ILLUSTRATIONS

Plate 1. Merozoites and trophozoites: note changes in nuclear configuration.

Figure 1. Fourth generation merozoites of Eimeria nieschulzi showing typical organelles: apical rings (ar), conoid (co), intravacuolar folds (if), micronemes (mn), parasite nucleus (n), rhoptries (r), and subpellicular microtubules (sm). X 15,000.

Figure 2. Early transitional stage: crescent body (bc), mitochondria (m), outer parasite membrane (ml), inner membrane of the merozoite (mi), nucleolus (nu), and parasitophorous vacuole (pv). X 19,000.

Figure 3. Early trophozoite with folded shape. Note the enlarged parasite mitochondria (m) compared to mitochondria of the host cell (double arrow) and of an uninfected cell (triple arrow). X 19,000.

Figure 4. Intermediate trophozoite. Degeneration of the host cell has occurred as indicated by short microvilli (v), convoluted host cell nucleus (nh), and a disruption of the cytoplasmic architecture (double arrow). X 10,600.

Figure 5. Late trophozoite containing numerous Golgi complexes (g) with associated dense cored bodies (single arrow), nuclear detachment bodies (nd), numerous small mitochondria (m), and segments of inner membrane (double arrow). X 9,400.

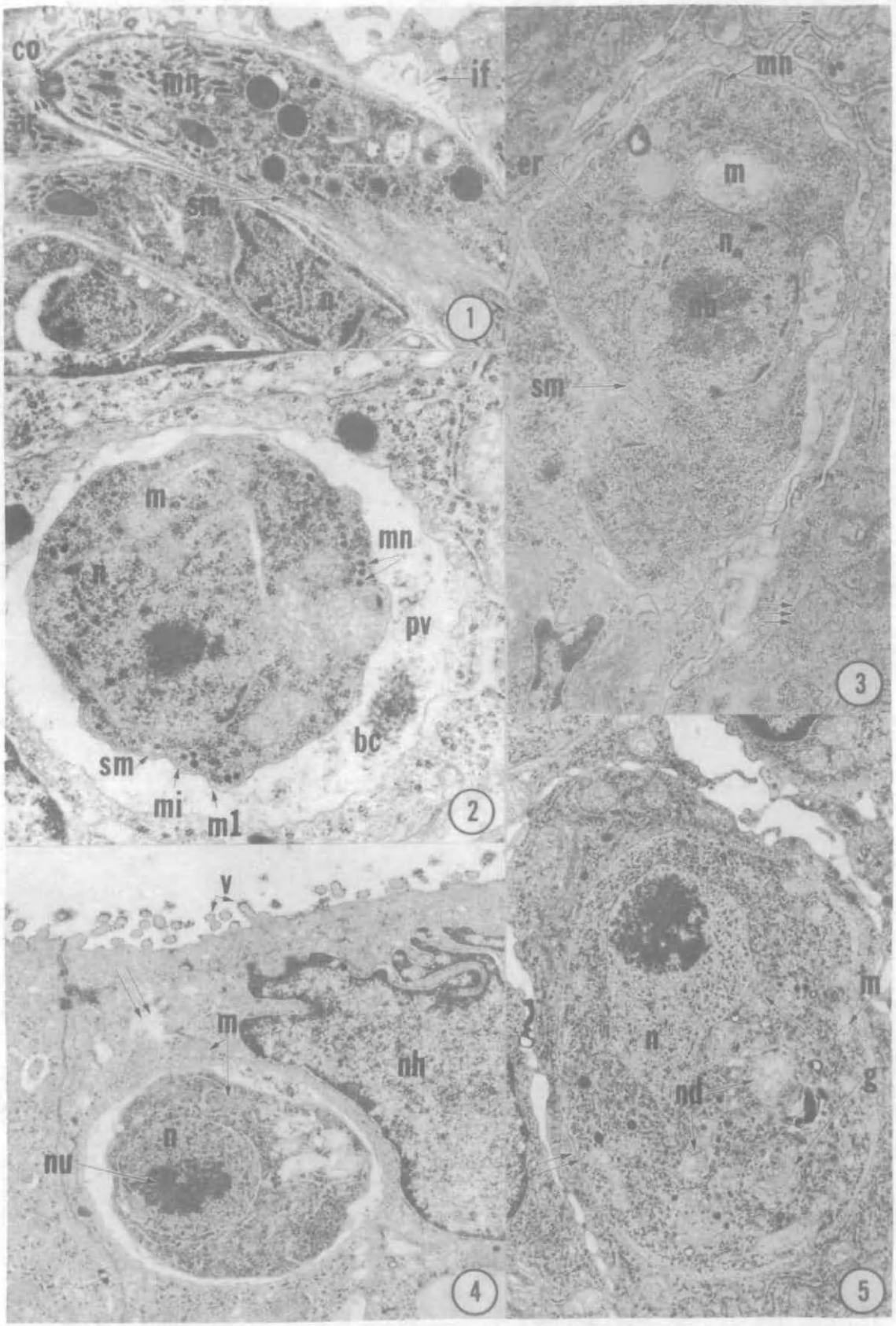
co
mn
if
sm
n
1
m
mn
n
pv
bc
sm
mi
m1
2
mn
er
m
n
nu
sm
3
v
m
nh
n
nu
4
m
n
nd
g
5

Plate 2. Early and intermediate macrogametocytes.

Figure 6. Earliest identifiable macrogametocyte with type 2 wall forming body (wf2) in the endoplasmic reticulum (er). Double arrow indicates an area of coarser chromatin. Single arrow indicates a dense cored body associated with a Golgi complex. X 9,400.

Figure 7. Inset from Fig. 6 showing an active micropore (mp) and crescent body (bc). Note the granular material resembling crescent body within the micropore saccule. The single arrow indicates a dense cored body. X 19,000.

Figure 8. An early macrogametocyte with developing wall forming bodies (wf2). A centriole (ce) is associated with a thickening of both membranes of the nuclear envelope. A Golgi complex (g) is associated with a ribosome-free area of the nuclear envelope. The double arrow indicates an area of coarser chromatin. X 9,400.

Figure 9. Condensation body (cb) of unknown composition. X 116,000.

Figure 10. Earliest intermediate macrogametocyte identified by amylopectin (ap) closely associated with endoplasmic reticulum (er). Note lipid body (lb), nuclear detachment bodies (nd), and segments of inner membrane (mi) at the parasite surface. X 8,200.

Figure 11. An intermediate macrogamont containing small amylopectin bodies (ap) and small lipid bodies (lb). X 7,700.

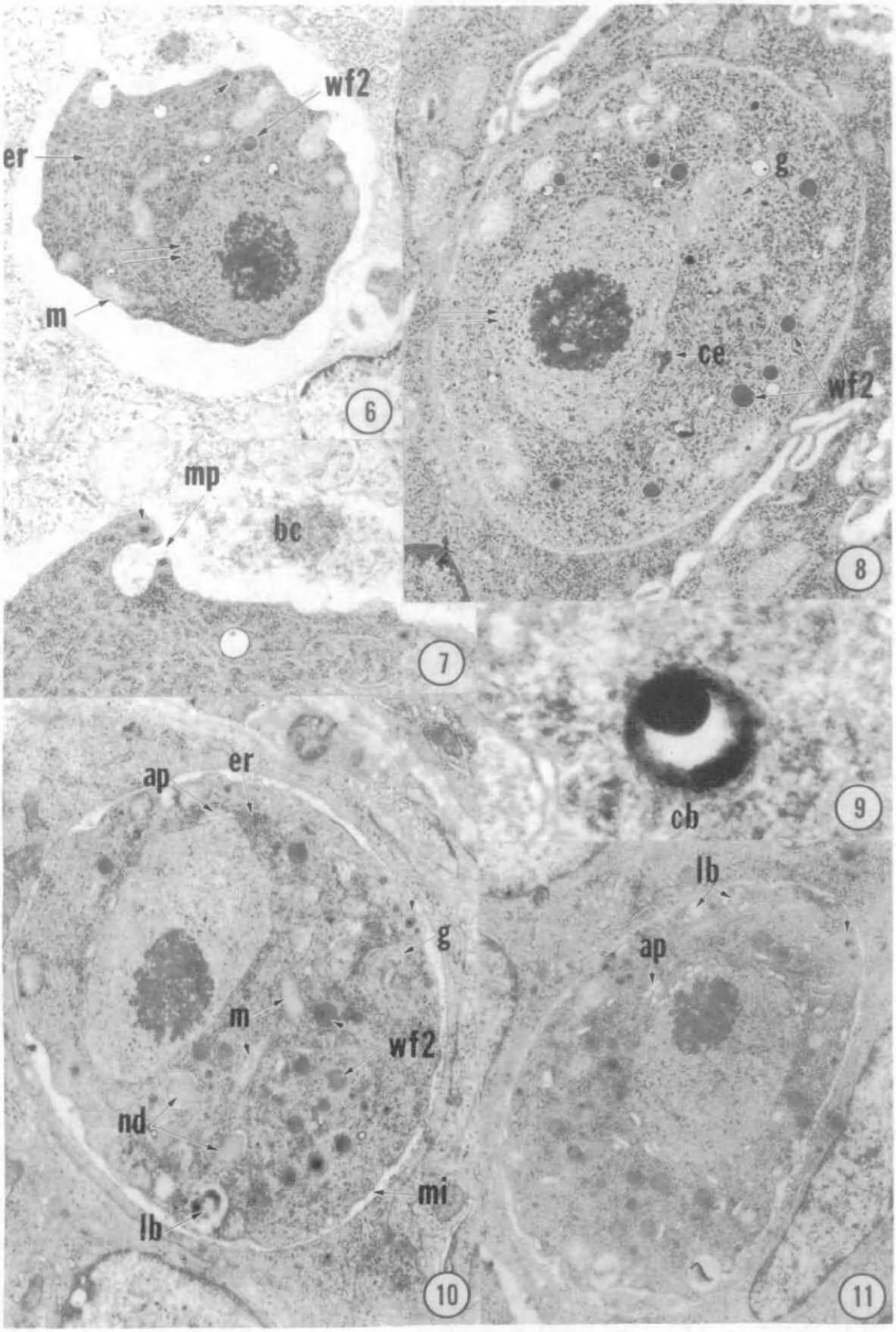
wf2
er
m
6
mp
bc
7
g
ce
wf2
8
cb
9
ap
er
g
m
wf2
nd
mi
lb
10
lb
ap
11

Plate 3. Zygotes.

Figure 12. Early zygote. The nucleus contains a dense chromatin inclusion (ni) and a tightly compacted nucleolus (nu). Note centrally located lipid bodies (lb), amylopectin (ap), and canaliculi (ca), and peripherally located wall forming bodies (wf1) and (wf2). Note that membrane m1 is detached and m2 limits the zygote cytoplasm. The host cell nucleus (nh) is distorted and displaced toward the intestinal lumen. Normal microvilli (v) of an uninfected adjacent intestinal cell can be seen at the upper right. X 6,200.

Figure 13. Inset of nucleus from Fig. 12 showing nucleolus (nu) and nuclear inclusion (ni). X 28,500.

Figure 14. Zygote showing rarefaction of the cytoplasm around wall forming bodies and granulation of wf1. X 9,400.

Figure 15. Wall forming bodies type 1 (wf1) and 2 (wf2) in an early zygote. Note the circular patterns of granulation of wf1. X 28,000.

Figure 16. Pattern B disintegration of wf2. A clear separation can be seen between m1 and m2. Note the vacuole around the wf2. X 19,000.

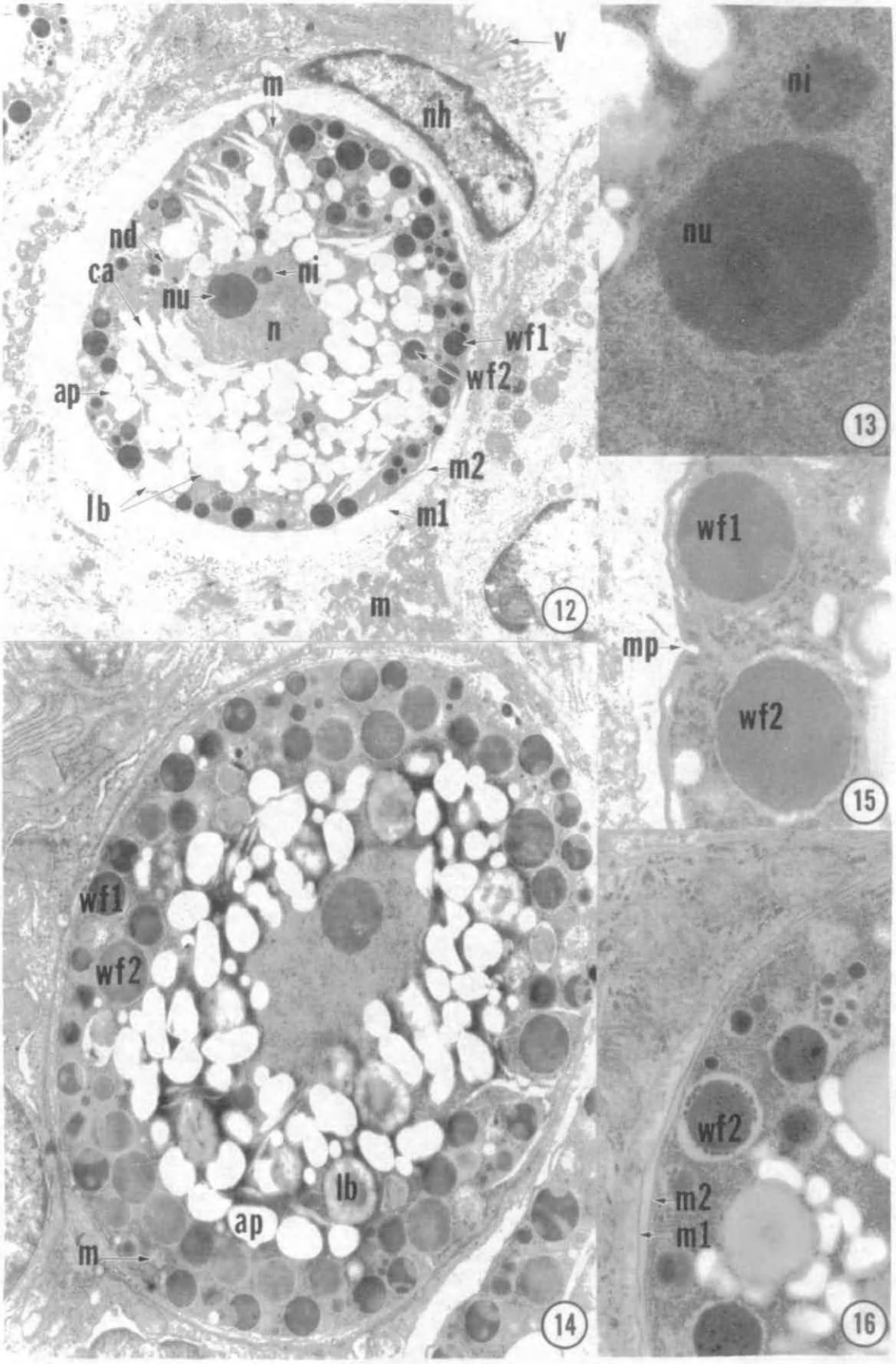
v
m
nh
nd
ca
ni
nu
n
wf1
wf2
ap
m2
lb
m1
m
12
ni
nu
13
wf1
mp
wf2
15
wf1
wf2
lb
ap
m
14
wf2
m2
m1
16

Plate 4. Early oocyst wall formation.

Figure 17. Pattern A disintegration of wf2 showing honeycomb density and coarse granules. Wf1 contain fine granules. Membranes m1, m2, and m3 are visible. X 19,000.

Figure 18. Zygote demonstrating Pattern A formation of the outer layer (wo) of the oocyst wall. Small dense granules at the periphery are residua of wf1 disintegration. Wf2 are labyrinthine. Peripheral mitochondria (m) are granule filled. X 6,600.

Figure 19. Inset from Fig. 18. Outer wall layer material has been deposited between membranes m2 and m3. Note disruptions in m3 (single arrows). Wall material covers a micropore (mp) in membrane m4 that is closely associated with electron lucent vesicles (vm). Note the close association of amylopectin bodies with the endoplasmic reticulum. X 19,000.

Figure 20. A subtangential section of pattern B outer wall layer formation. Granules and condensed wall material are shown outside membranes m3 and m4. Note that the membranes that surround two wf2 have fused to form a larger vacuole (*). X 19,000.

Figure 21. Zygote demonstrating pattern B outer wall layer formation. Amylopectin bodies (ap) are slightly reduced and are located at the margins of lipid bodies (lb). One mitochondrion (m) is associated with the nucleus. Microgametes (mg) are present in an adjacent cell. X 8,300.

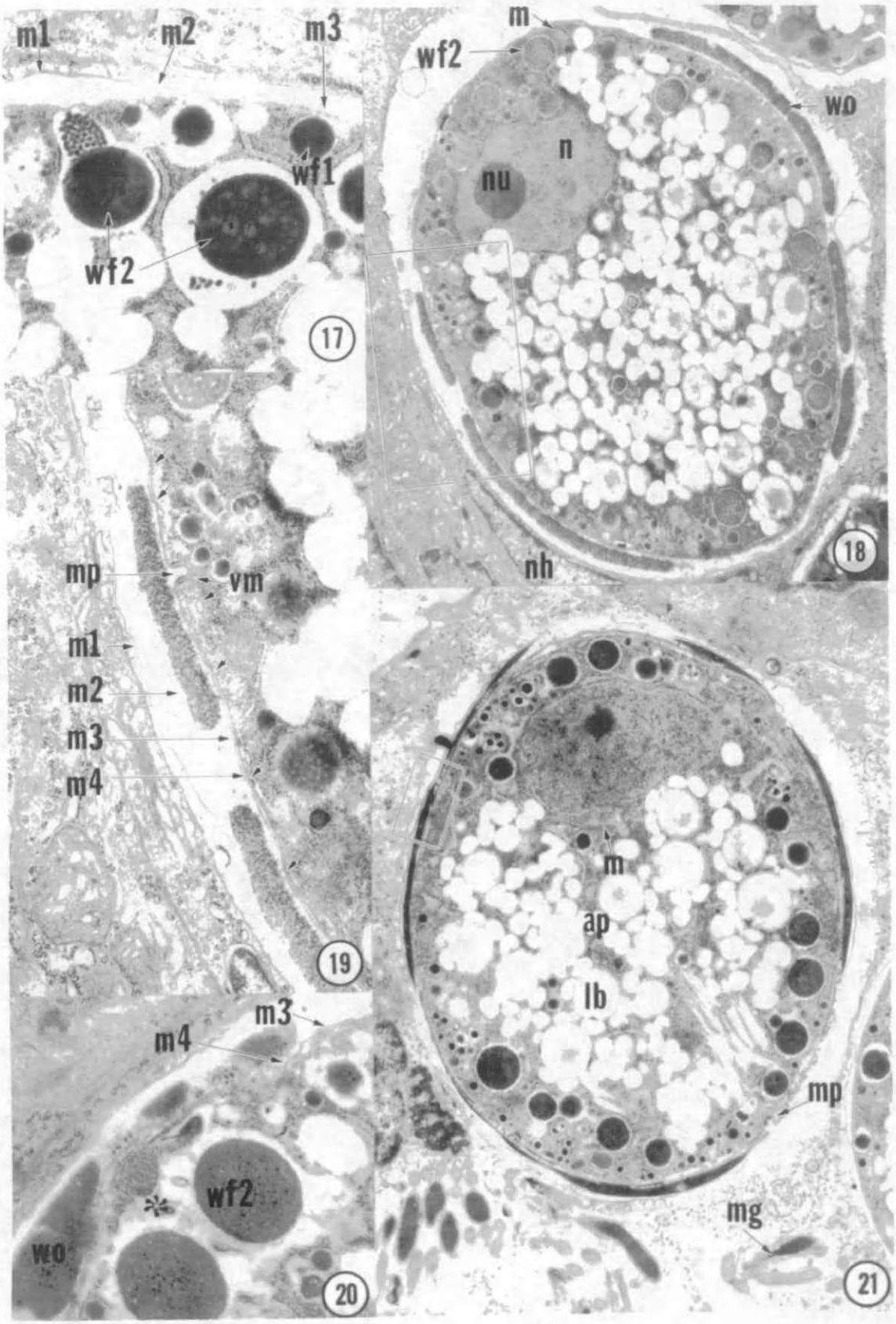
m1
m2
m3
wf1
wf2
17
mp
vm
m1
m2
m3
m4
19
m3
m4
wf2
wo
20
m
wf2
wo
n
nu
nh
18
m
ap
lb
mp
mg
21

Plate 5. Oocyst wall formation.

Figure 22. Inset from Fig. 21 showing a stage in pattern B formation of the outer wall layer. Membrane m3 appears to end at the arrow. X 56,000.

Figure 23. Zygote demonstrating pattern C inner wall layer formation. Membranes are extensively folded. Spherical electron dense bodies (db) are present in the cytoplasm and between membranes m4 and m5. X 9,400.

Figure 24. High magnification of pattern C inner layer formation from a serial section of Fig. 23. Outer wall layer (wo) shows differential condensation with higher density in the medial portion. Inner layer material (wi) is well demarkated and homogeneous. Exocytosis of wi material is suggested at the double arrow. Small globules of material beneath m5 (single arrows) have the same density as spherical dense bodies (db). X 12,500.

Figure 25. High magnification of pattern C inner layer formation. Outer layer is not yet formed above the portion pictured. The inner layer (wi) is finely granular and less dense that in Fig. 24. A dense flattened body immediately beneath m5 is of identical density to a spherical dense body (db) under m6. X 21,200.

Figure 26. High magnification of pattern D inner layer formation. Outer layer (wo) is coarsely granular and more dense at the medial surface. The lucent layer (ll) is uniform and separates wo from the forming, globular inner layer (wi). Membranes m5, m6, and m7 lie beneath the forming inner layer. Haloed dense bodies (db) and labyrinthine wf2 are present in the peripheral cytoplasm. Canaliculi (ca) extend to m7. X 21,200.

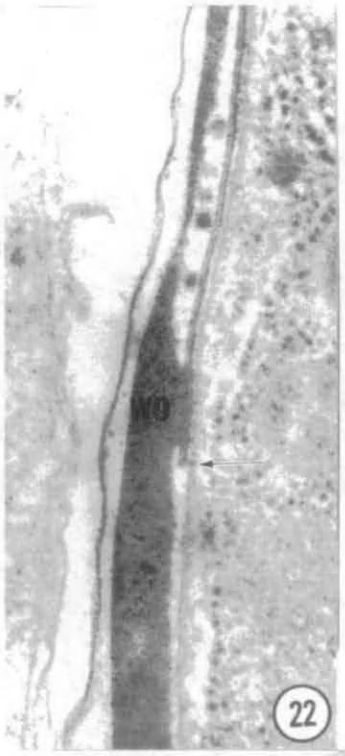
wo
22

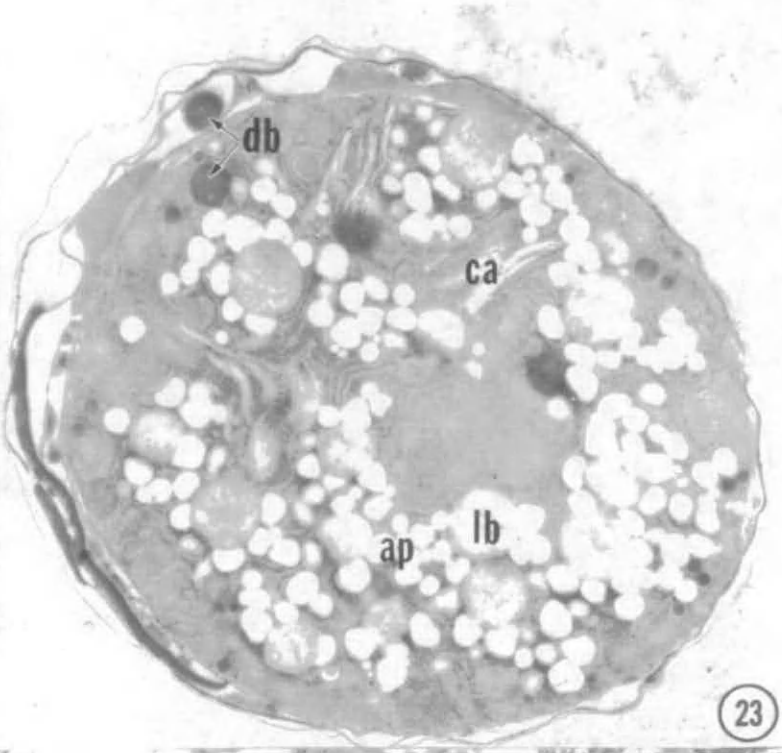
db
ca
ap
lb
23

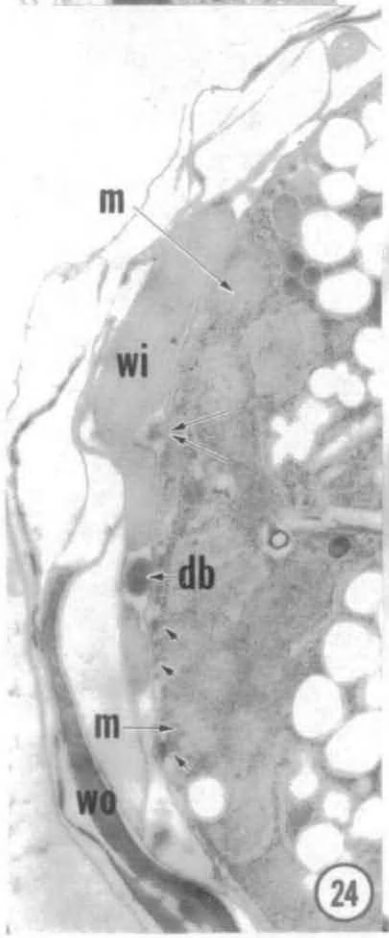
m
wi
db
m
wo
24

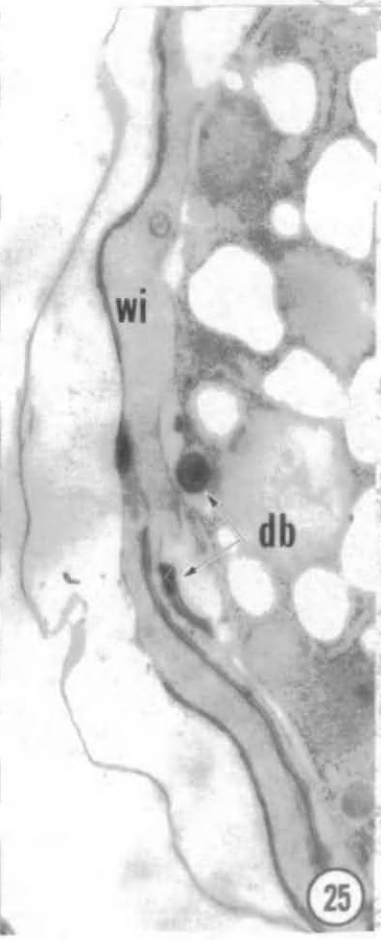
wi
db
25

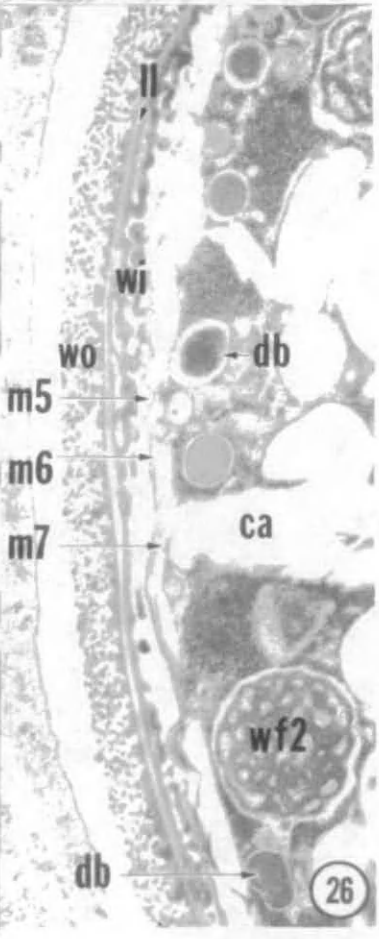
ll
wi
wo
db
m5
m6
m7
ca
wf2
db
26

Plate 6. Wall formation and formed oocysts.

Figure 27. Pattern D wall formation with the inner layer coalescing at its distal surface. An electron dense layer (dl) lies beneath m7 and forms a loop into the peripheral cytoplasm. X 9,400.

Figure 28. Oocyst sectioned through the nucleus and nucleolus (nu). The inner wall layer (wi) has separated from the outer layer (wo). The nucleus and nucleolus are similar to those of the late microgametocyte. X 6,200.

Figure 29. Mature oocyst with the condensed sporont and a fluid filled space (fs). Membrane m2 appears detached from the outer surface in some areas. Micropyle is at lower right. X 10,600.

Figure 30. Macrogametocyte and zygote within the same parasitophorous vacuole (pv). Zygote (Z) is in the process of wall formation. The host cell nucleus (nh) is extremely convoluted. Microvilli (v) of the host cell are sparser than those of the uninfected adjacent cell. X 6,300.

Figure 31. Complete oocyst wall of an intact oocyst. The outer layer (wo) is electron dense and granular. The lucent layer (ll) corresponds to the membranous complex m3-m4. The inner layer (wi) is of moderate density and uniform thickness. Membranes are not well visualized due to nonperpendicular plane of section and inadequate fixation beneath the outer wall layer. X 70,000.

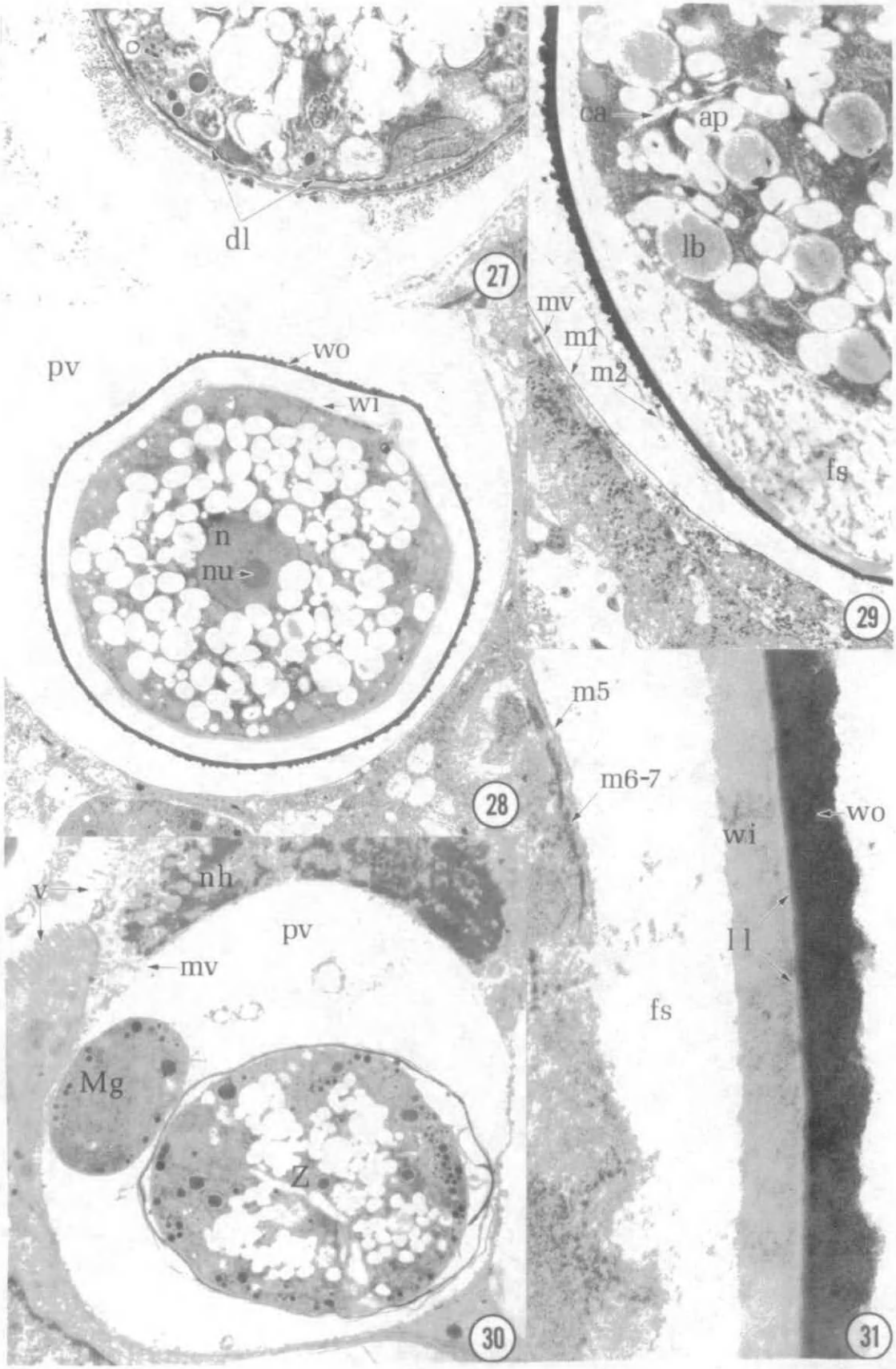
dl
27
ca
ap
lb
mv
m1
m2
fs
29
pv
wo
wi
n
nu
28
m5
m6-7
wi
wo
v
nh
pv
mv
ll
fs
Mg
Z
30
31

Plate 7. Early microgametogenesis.

Figure 32. Early microgametocyte with an elongate nucleus (n) and a rod shaped nucleolus (nu). The nuclear envelope (ne) is intact. Double arrows indicate separate areas of coarse chromatin. Note the presence of certain residual merozoite organelles; microneme (mn) and inner membrane (mi). A small crescent body (bc) is present in the parasitophorous vacuole. X 10,600.

Figure 33. Binucleate microgametocyte in degenerate host intestinal epithelium. Microvilli (v) of the brush border are sparse and short. Epithelial cells are reduced to low cuboidal or squamous. A capillary is distended and contains few red blood cells (rbc). X 2,700.

Figure 34. Inset from Fig. 33 showing the dividing nucleus. The nucleolus (nu) is dumbell shaped. The nuclear envelope (ne) is intact and somewhat constricted at the center. Certain parts of the mitotic apparatus are visible; centriole (ce), centrocone (cc), and radiating spindle microtubules (st). X 19,000.

Figure 35. Young microgametocyte with four nuclei in the plane of section. Note extensive mitochondria (m), Golgi complexes (g), and endoplasmic reticulum (er). Some parasite nuclei are in contact with the surface membrane at points of contact with the parasitophorous vacuolar membrane (mv) (arrows). X 9,400.

Figure 36. Serial section of dividing nucleus in Fig. 35 inset. Note kinetochore (k) at the end of a spindle microtubule (st). The nuclear envelope (ne) is intact. X 56,000.

Figure 37. Serial section of Fig. 36. A centriole (ce) and centrocone (cc) lie within the plane of section. Some spindle microtubules (st) extend past the chromatin at the metaphase plate. X 56,000.

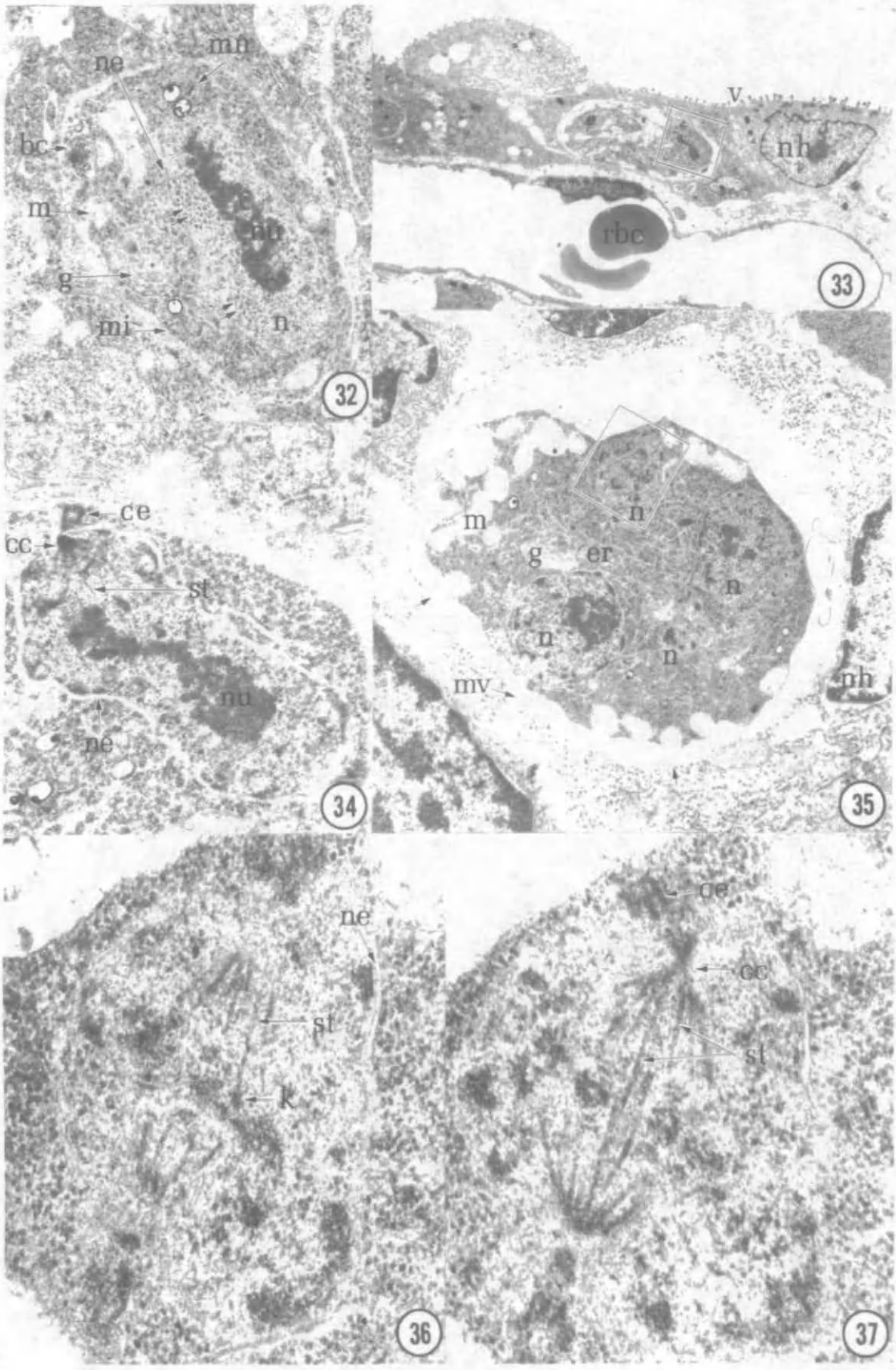
ne
mn
bc
m
g
mi
n
32
v
nh
rbc
33
ce
cc
st
nu
ne
34
m
n
g
er
n
n
n
n
mv
nh
35
ne
st
k
36
ce
cc
st
37

Plate 8. Development of microgametocytes.

Figure 38. Intermediate microgametocyte with multiple peripheral nuclei without nucleoli. Mitotic spindles (s) are present in two nuclei. A late macrogamete (Mg) is present in an adjacent cell. X 6,700.

Figure 39. Dumbell shaped nucleus from inset in Fig. 38. Three centrioles (ce) are within the plane of section. Note the close association of centrioles with the surface membrane, the deep indentation of the nuclear envelope near the centrioles, and the dense chromatin at the periphery of the nucleus. X 38,000.

Figure 40. Intermediate microgametocytes showing deep surface invaginations. Nuclei occur throughout the gametocyte. Note mitotic spindles (s) in several nuclei, a typical micropore (mp) and marked thickenings of the surface membrane above several pairs of centrioles (double arrows). X 9,400.

Figure 41. Mature microgametocyte showing nuclear chromatin condensation and formation of flagella (f). Note amylopectin (ap) and lipid bodies (lb) in the endoplasmic reticulum (er). A late macrogamete is present in an adjacent cell. X 5,300.

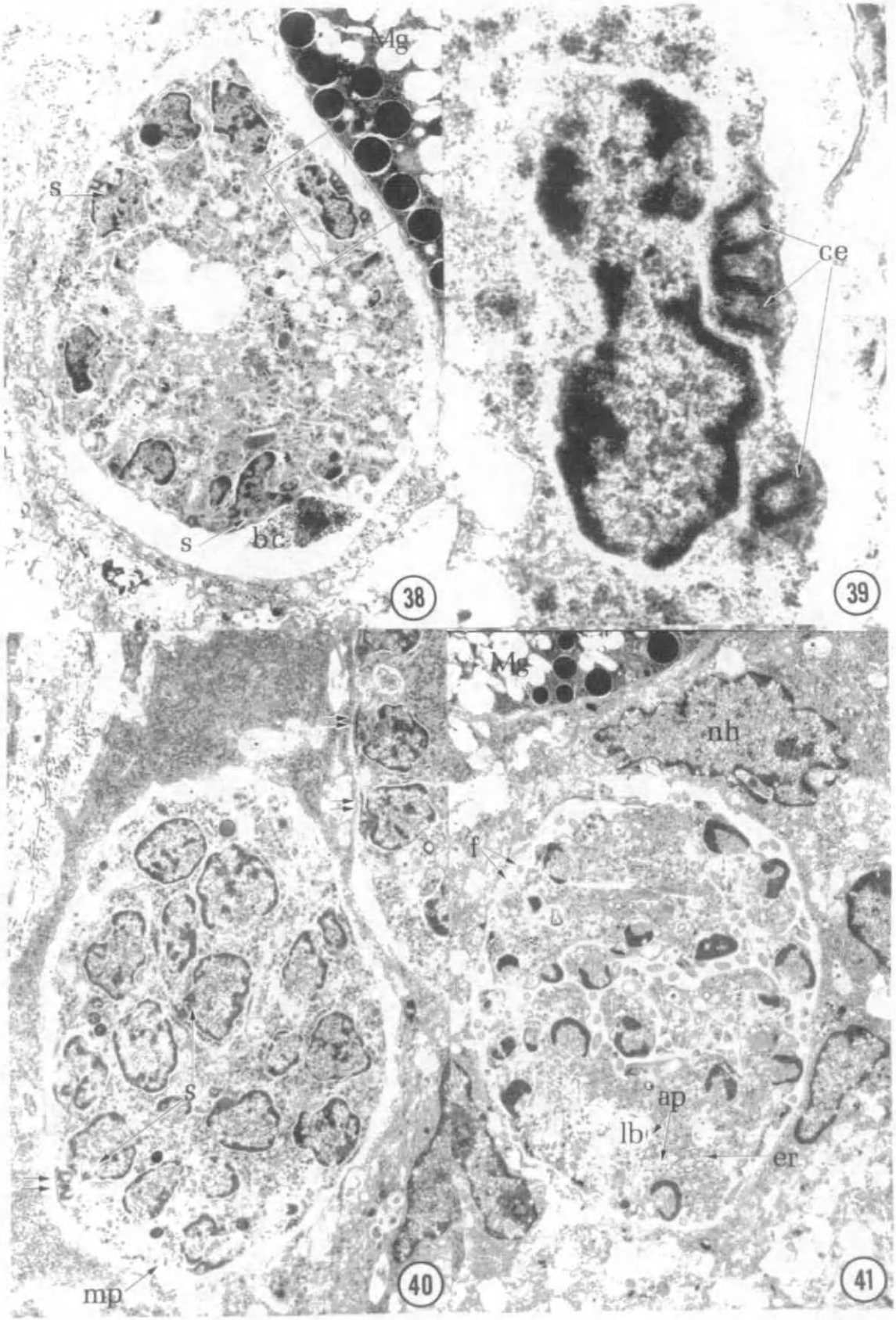
Mg
s
s
bc
38
ce
39
Mg
nh
f
ap
lb
er
s
mp
40
41

Plate 9. Mature microgametocytes and microgametes.

Figure 42. Nucleus (n) with condensing chromatin and flagellar apparatus: Basal body (bb), flagellar rootlet (rf), and flagellum (f). X 56,000.

Figure 43. Mature microgametocyte with budding microgametes, which have long flagella. Nuclear chromatin is condensed (nc), and mitochondria (m) are closely associated with each nucleus. A lipid body (lb) is surrounded by small amylopectin bodies. X 7,900.

Figure 44. Budding microgamete at the surface of the microgametocyte. Note numerous flagella (f), the dense ring (dr) containing microtubules (mt), the nuclear residuum (nr), and condensed nuclear chromatin (nc). X 23,800.

Figure 45. Cross section through a completely formed microgamete. The condensed nucleus (nc) is coarsely granular and surrounded by a nuclear envelope (ne). Three microtubules (mt) are visible in the body of the microgamete. A single limiting membrane (ml) has a fine granular substance at the distal surface. X 84,000.

Figure 46. Sagital section through a completely formed microgamete showing a condensed nucleus (nc), mitochondrion (m), body microtubules (mt), a flagellum (f) with its basal body (bb), and perforatorium (p). X 28,500.

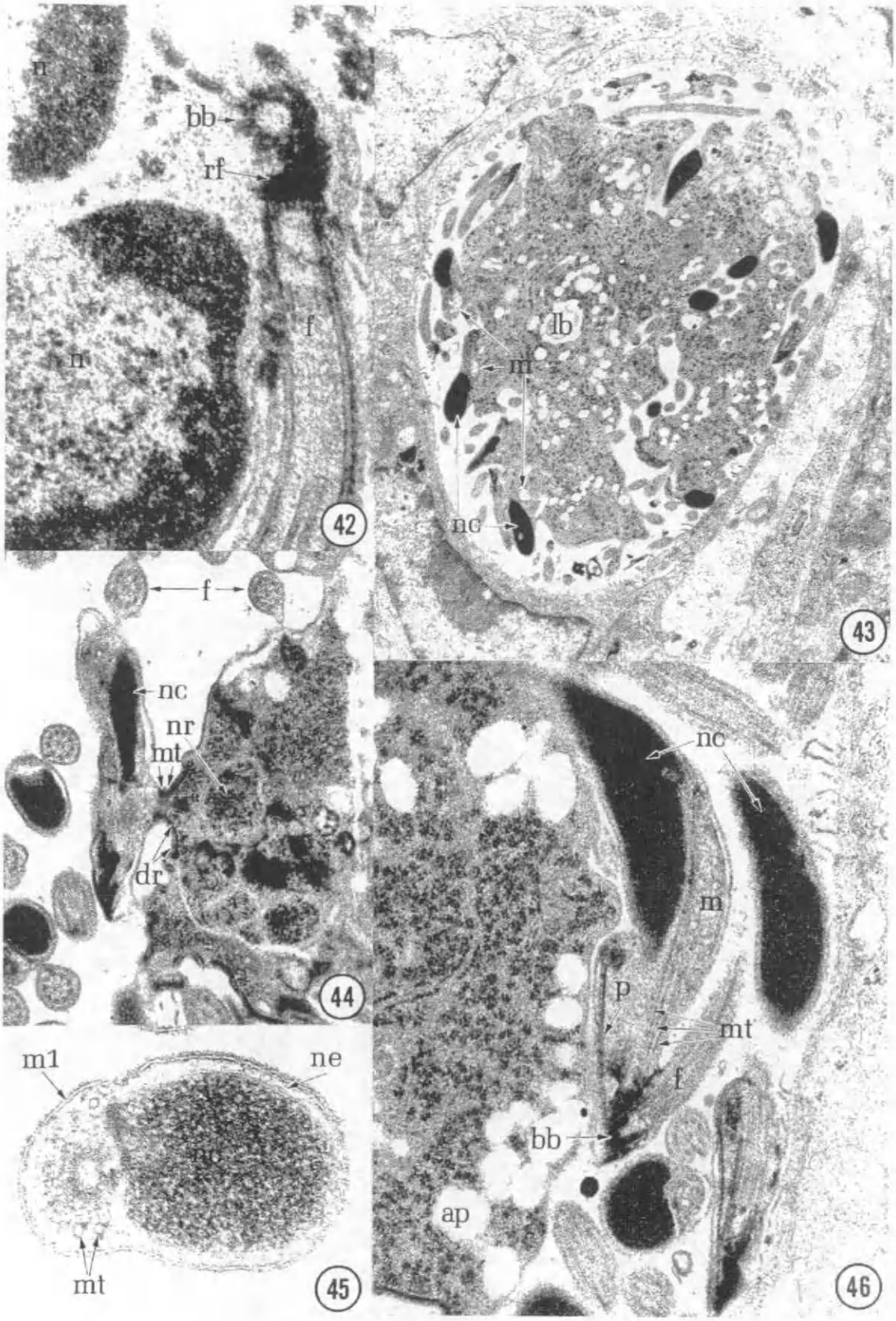
n
bb
rf
f
m
42
lb
m
nc
43
f
nc
nr
mt
dr
44
nc
m
p
mt
f
bb
ap
46
m1
ne
mt
45

Plate 10. Mature microgametes.

Figure 47. Microgamete flagella (f) in cross section. Note the microtubular arrangement of nine pairs around two unpaired microtubules in most sections and unpaired microtubules in sections near the flagellar tips. X 56,000.

Figure 48. Mature microgametes in the parasitophorous vacuole and the microgametocyte residuum (MR). Dense rings (dr) occur at the surface of the residuum. Nuclear residuua (nr), mitochondria (m), and amylopectin (ap) appear within the microgametocyte residuum. X 7,000.

Figure 49. The anterior tip of a mature microgamete showing the apex of the perforatorium (p), a flagellar rootlet (rf), basal body (bb), and flagellum (f). Note the foamy appearance of the host cell cytoplasm containing parasite flagella (f) at top. X 21,400.

Figure 50. A host cell nucleus (nh) penetrated by a microgamete (mg). A zygote (Z) is present in the adjacent cell. Note the pyknotic character of the penetrated nucleus compared to the adjacent host nucleus. X 10,600.

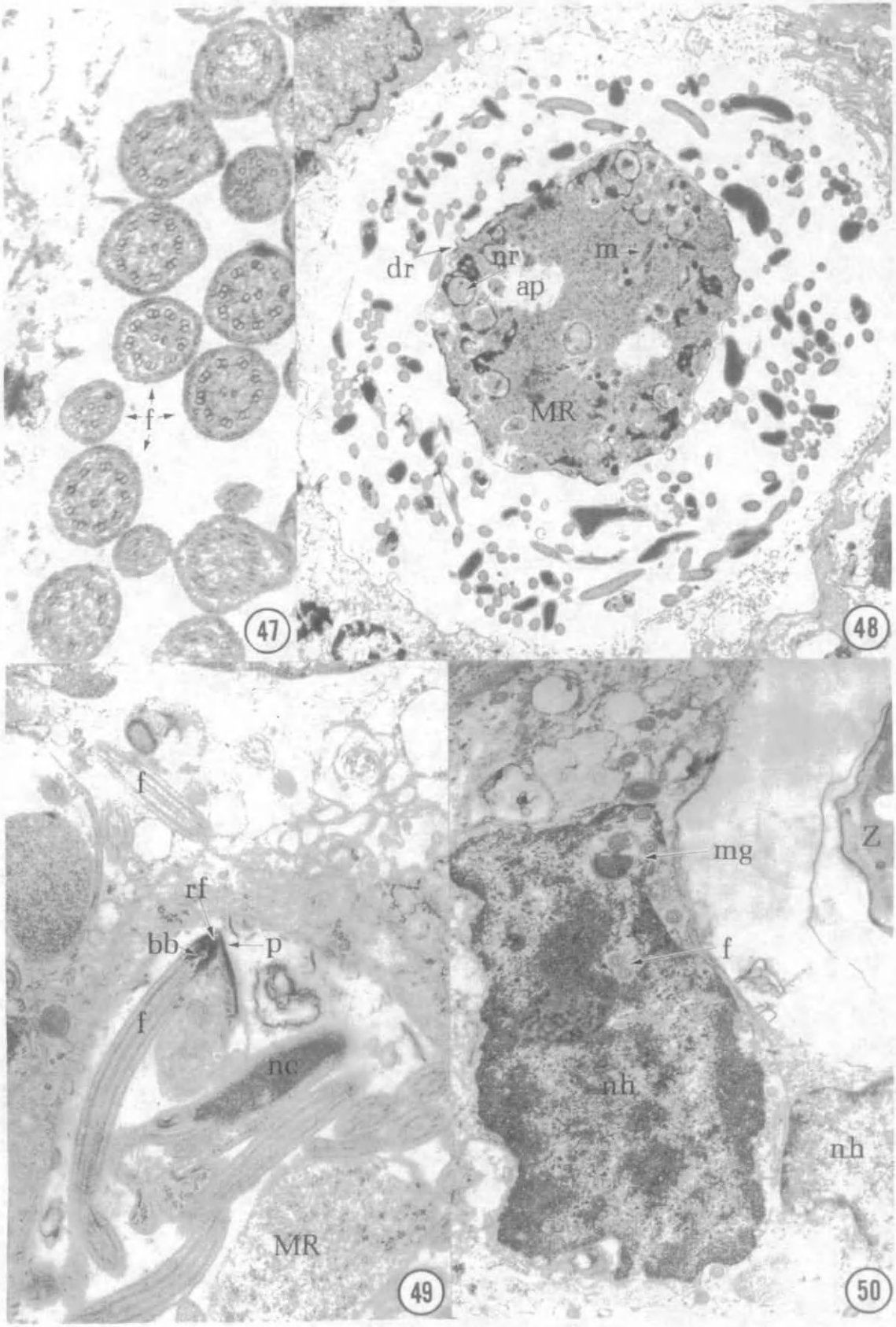
f
dr
nr
ap
m
MR
47
48
f
rf
bb
p
f
nc
MR
49
mg
Z
f
nh
nh
50

# DISCUSSION

The sexual stages of eimerian parasites develop from merozoites of apparently mitotic origin. Although there is considerable controversy in the literature as to which stage undergoes meiosis, it is agreed that late merozoites are sexually differentiated on the basis of differential PAS staining and nuclear configuration (28, 34, 58). In Eimeria nieschulzi, gametogony follows four generations of schizogony (33, 41). Although other authors have reported young trophozoite stages to be sexually distinguishable by nuclear and cytoplasmic configuration in E. magna (61) and E. brunetti (12), macrogametocytes of E. nieschulzi were not identified positively until distinctive cytoplasmic inclusions were present.

## Macrogametocytes

The earliest identification of macrogametocytes of E. nieschulzi was made by the presence of type 2 wall forming bodies (wf2) within cisternae of the endoplasmic reticulum as reported for E. mivati (70), E. ferrisi (6), and E. tenella (48, 56). The wf2 appeared to arise entirely within the rough endoplasmic reticulum (RER) as reported in E. ferrisi (6) and E. labbeana (66). No association was observed between wf2 and Golgi complexes as reported in E. acervulina (27), E. brunetti (12), and E. mivati (70). The wf2 were quite homogeneous in young macrogametocytes, showing only a fine granular structure as in E. magna (61), E. brunetti (12), E. falciformis (51), Isospora spp. (48), and Toxoplasma gondii (48). These were quite unlike the honeycombed or

labyrinth bodies reported in all other eimerian species studied, including the early study of E. nieschulzi (7). This difference may be due to fixation and preparation procedures. The wf2 in E. nieschulzi assumed a honeycombed appearance that turned to labyrinthine as the bodies were broken down for wall formation. The type 2 wall forming bodies (wf2) appeared earlier than type 1 (wf1) in E. nieschulzi as reported in all eimerian species studied except E. magna, in which the two types appeared to arise simultaneously. In E. nieschulzi, the wf2 were consistently larger than wf1 with the former reaching a maximum diameter of 1.06 um and the latter about 0.94 um. This is consistent with observations in E. acervulina (27), E. auburnensis (50), E. bovis (50), E. falciformis (51), E. ferrisi (6), E. intestinalis (60), and E. magna (61). The wf1 were larger than wf2 in E. brunetti (12), E. maxima (36), E. perforans (45), E. steidai (50), and E. tenella (48, 56). The wf1 and wf2 were of equal size in E. mivati (70).

As reported in all other eimerian species studied, the wf1 lay peripheral to wf2, the former were more electron dense than the latter, and only the wf1 appeared membrane bound. Wf2 always lay within cisternae of RER. The origin of wf1 is still not clear; coalescence in the cytoplasm of small membrane bound osmiophilic granules of Golgi origin was reported in E. acervulina (27); formation directly from Golgi complexes was reported in E. mivati (70); and wf1 were reported to arise within peripheral mitochondria in E. falciformis (51), E. labbeana (66), E. maxima (36), and E. perforans (45). In E. nieschulzi the wf1 appeared free in cytoplasm and not associated with other organelles.

Presumably after fertilization, the wf1 began to break down, forming crescent or circular areas of granularity of lower electron density than homogeneous areas. The curved boundaries suggested spreading of the granularization from a pointwise addition of an enzyme. A similar pattern is seen in micrographs in an earlier study of E. nieschulzi (7), but not in any other eimerian species studied. In E. bovis (50) and E. mivati (70), the wf1 appeared to break down by irregular fracturing with accompanying vacuole formation. As wf1 in E. nieschulzi diminished in size, there was only 2 narrow surrounding vacuoles formed and no fusion of the bodies. By the time deposition of the outer wall layer commenced, the wf1 were reduced to extremely electron dense granules.

In the present study, wf2 of E. nieschulzi began to break down before deposition of the outer wall layer. Granules of about 50 nm in diameter were observed at the surfaces of wf2 or in the extensive vacuoles that temporarily formed around these bodies. Vacuoles surrounding adjacent wf2 fused so that several wf2 occurred within a common vacuole similar to that reported in other eimerian species. However, wf2 did not fuse with each other as in E. bovis (50), E. labbeana (66), and E. magna (61); nor did they fuse with the inner limiting membrane as reported in E. acervulina (27). Scholtyseck and Voigt (54) and Lee and Millard (27) stated that wf1 fused with the inner membrane and released their contents between membranes 1 and 2 to form the outer wall layer, then wf2 similarly fused to form the inner layer. Seliverstova (57) suggested that material from both wf1 and wf2 combined to form the outer wall layer and material from

wf2 alone comprised the inner layer. Scholtyseck (46) reported that the outer layer was made of fused material from breakdown of wf1 and the inner layer was from coalescence of wf2. In E. nieschulzi, there was transport of fine granular material from breakdown of wall forming bodies across one intact membrane, m4, and one partially discontinuous membrane, m3, to a space between membranes m2 and m3 where it coalesced to form the outer wall layer. The partial breakdown of wf2 before deposition of the outer layer lends support to Seliverstova's contention of material from both types of wall forming body being incorporated into the outer wall layer (57). The appearance of 50 nm particles, similar to those formed during early wf2 breakdown, in the uncoalesced outer layer also tend to support that hypothesis. Since no specific histochemical labeling has been performed on the substances from wf1 and wf2, it is not possible to state whether material from wf2 is or is not included in the outer layer of the oocyst wall. Nor is it possible to state positively that the inner wall layer is made entirely of material from wf2. The observation of spherical bodies or irregular globules of higher electron density beneath membrane m6 or associated with the wf2 may have been modified or supplimented prior to incorporation into the forming inner layer. The material forming the inner layer was transported or exocytosed into the space between membrane complex m3-m4 and m5-m6 either as fine granular material or as globules. Only small spherical residue of wall forming bodies remained in the sporont after completion of the oocyst wall.

Macrogametogenesis and subsequent oocyst wall formation involved extensive membrane proliferation in E. nieschulzi. The trophozoite

stage had a single limiting membrane with underlying segments of a closely applied membrane presumed to be residua of the inner membrane complex of the merozoite or possibly newly synthesized membrane. This observation is consistent with reports of all other eimerian macrogametogenesis studies except of E. maxima (36) in which 2 complete membranes were observed in trophozoites. Mature macrogametes of E. nieschulzi were earlier reported as single membrane bound (7). Scholtyseck (46) reported that macrogametes of E. falciformis, E. perforans, E. stiedai, and E. tenella were limited by a single membrane with an underlying osmiophilic mass. Mature macrogametes of E. nieschulzi are limited by two closely applied membranes, as reported in E. acervulina (27), E. bovis (50), E. intestinalis (60), E. labbeana (66), E. magna (61), and E. maxima (36). A triple limiting membrane was reported in mature macrogametes of E. auburnensis (50), E. brunetti (12), E. ferrisi (6), and E. mivati (70); and after fertilization in E. acervulina (27). A fourth membrane was suspected to appear during oocyst wall formation in E. acervulina (27). Five membranes were reported in wall forming stages of E. perforans (52) and E. tenella (57). The process of oocyst wall formation was observed in greater detail in this study than in any others previously reported. Seven membranes were distinguishable in the formation of oocysts of E. nieschulzi. Membrane m3 appeared after fertilization and before breakdown of type 2 wall forming bodies (wf2). Membrane m4 appeared prior to deposition of the outer wall layer. Material forming the outer wall layer was evidently transported across the innermost membrane, m4, and the partially incomplete m3. The original trophozoite

membrane, m1, was loosely attached to the surface of the zygote; m2 bounded the forming outer layer of the oocyst wall at the distal surface; and the membrane complex m3-m4 bounded the outer layer at the proximal surface. Membrane 5 was laid down immediately prior to deposition of the inner wall layer and constituted the proximal limit of that forming layer, the distal limit being membrane complex m3-m4. Small spherical bodies were apparently exocytosed across m5 and fine granular material may have been extruded from openings in m5. Membrane 6 became closely associated with m5 prior to completion of the inner wall layer while m7 appeared to be separated from m5-m6 at most points. The observed positions of the innermost membranes suggested that membrane complex m5-m6 became adherant to the innermost surface of the oocyst wall and m7 was the limiting membrane of the sporont.

Nuclear changes in E. nieschulzi during dedifferentiation from the merozoite to the trophozoite and during macrogametogenesis quite closely followed those reported in all other eimerian species studied. The nuclear configuration changed from one of coarse, densely clumped peripheral chromatin and very diffuse nucleolus in merozoites to one of a slightly condensed nucleolus and fine granular euchromatin with an area of coarser heterochromatin in late trophozoites and early macrogametocytes. Mature macrogametes had very fine grained and uniform nucleoplasm with a single spherical, highly condensed nucleolus. Zygotes showed a much less distinct nuclear envelope but similar internal fine structure to the nucleus of mature macrogametes, with the exception of a second dense spherical inclusion in several specimens that was distinctly chromatinous as opposed to nucleolar. A similar

structure has been reported only in late macrogametes of E. brunetti (12). Complete serial sections of most zygote nuclei were not available in this study to determine whether all such nuclei contained the inclusion. The structure is of unknown significance, but might represent the nucleus of a microgamete after fertilization. The only report of a microgamete appearing within a macrogamete in coccidia was made by Scholtyseck and Hammond (49) in which a complete microgamete was observed in the cytoplasm of a macrogamete of E. bovis. Neither penetration of a macrogamete by a microgamete nor fusion of gamete nuclei in coccidia have been reported.

Certain other inclusions characteristic to coccidian macrogametocytes were also observed in E. nieschulzi. Inclusions that were bound by a double membrane, contained in an amorphous granular substance, and lay close to the nucleus were called 'nuclear detachment bodies' in E. mivati (70) and E. brunetti (70). Similar bodies in E. magna (61) were termed "Golgi adjuncts" to be consistent with terminology in an earlier study of Toxoplasma gondii (61). Such bodies in E. brunetti, E. magna, and E. mivati macrogametocytes appeared to be areas of pinched off nucleoplasm or finger-like projections thereof. Similar bodies in a more recent study of E. brunetti macrogametocytes (12) were termed "multimembranous vesicles" due to uncertainty of their origin. Although the contents of such bodies in E. nieschulzi did not appear identical to nucleoplasm, the term "nuclear detachment body" was considered preferable.

Characteristic electron lucent inclusions have been shown to be polysaccharide by periodic acid-Schiff staining for light microscopy

(43) and by periodic acid thiocarbohydrazide-silver--protein staining for electron microscopy (6, 65). Ryley et al. (44) reported such polysaccharide extracted from mixed endogenous stages of E. tenella and E. brunetti to be amylopectin. Most recent literature on coccidian ultrastructure refers to such inclusions as amylopectin bodies. In E. nieschulzi, the amylopectin first appeared as electron transparent rod shaped bodies about 0.3 by 1.0 um between layers of endoplasmic reticulum and along the outer nuclear membrane as reported in E. magna (61) and E. brunetti (12). Electron dense rod shaped granules identified as amylopectin in E. mivati (70) were not observed, nor were small osmiophilic vesicles seen associated with typical appearing amylopectin bodies, as in E. acervulina (27). In zygotes and early oocysts, the amylopectin bodies were almost entirely associated with large lipid bodies. This observation is consistent with an earlier report in E. nieschulzi (7) that 'glycogen' bodies were only associated with 'vacuoles' and not other membranes. No other species studied has shown this degree of association between the amylopectin bodies and lipid bodies.

Associated with Golgi complexes in late trophozoites and early macro- and microgametocytes were small bodies about 0.2 um in diameter with denser cores. Such bodies were much more numerous in macrogametocytes than in microgametocytes. Speer et al. (61) reported Golgi complex associated vesicles containing particulate matter and dense cores in macrogametocytes of E. magna, and suggested they represent the anlage of lipid bodies. The observation that dense cored bodies disappeared when characteristic lipid bodies appeared furthers the

suggestion that lipid bodies arise, at least in part, from Golgi complexes.

Eclipse-like condensation bodies with an average outside diameter of 210 nm and core diameter of 95 nm were seen in all stages of E. nieschulzi except microgametes as well as within a number of intestinal spirochetes, but never in host tissue. Such structures undoubtedly represented condensed areas of some substance in the cytoplasm of non-mammalian cells, but neither the condensed substance nor the process inducing such condensation is known. Similar inclusions are evident in electron micrographs of virtually all species of Eimeria studied ultrastructurally.

The parasitophorous vacuole (pv) surrounding coccidian parasites is limited by a single membrane from the host cell. The vacuole membrane was highly convoluted in most specimens with numerous intravacuolar folds up to 530 nm in length, which often were in contact with ml. Such folds were characteristic of the pv of all Eimeria species studied, but occurred in different numbers and with different lengths in the various species (52).

Intravacuolar tubules up to 90 nm in diameter have been reported in the pv of macrogametocytes of E. auburnensis (50), E. bovis (50), E. brunetti (12), E. labbeana (66), E. falciformis (51), E. magna (61), E. maxima (36), E. mivati (70), E. perforans (45), E. nieschulzi (7), and E. tenella (48) and 'vesicles' with subunit type walls were observed in E. acervulina (27). Scholtyseck stated, "Probably, such tubules are characteristic of all macrogametes of Eimeria species." In E. labbeana, intravacuolar tubules were observed in about 0.1% of macrogametocytes

(66). Intravacuolar tubules were not observed in E. ferrisi (6), E. intestinalis (60), E. stiedai (50), or in the present study of E. nieschulzi.

It is generally believed that nutrition of the parasite involves the structures within the parasitophorous vacuole and surface structures in the plasmalemma (46). "Inactive" micropores were present in low numbers in most macrogametocytes of E. nieschulzi, as in all other species studied. A few specimens had "active" micropores with a large internal fluid filled saccule which contained a granular substance resembling that present in the pv. In such specimens the granular material was localized within the pv into a loosely organized crescent body. This association might suggest that these micropores functioned as a cytopyge or excretory pore rather than a cytostome, as commonly assumed (46). Micropores were also present in membrane 4 during deposition of the outer layer of the oocyst wall. Small electron lucent vesicles lay close to such micropores in the cytoplasm. The function and significance of micropores in inner membranes are unknown, but their presence suggests that the membrane is active in transport of materials. Micropores were not present in outer membranes.

Deep invaginations in the pellicle of early macrogametocytes of E. auburnensis (50), E. intestinalis (60), and E. nieschulzi (7) were reported to function in pinocytosis. Similar invaginations were observed in a small percentage of young macrogametocytes in the present study, but pinocytotic vesicles were not present. Trophozoites and early gametocytes had a granular substance within the pv that resembled a loose crescent body in some specimens. Kelly and Hammond (25)

reported that the granular substance in E. ninakohylakamovae schizonts originated from material derived from the host cell, probably by the pinching off of outpocketings or folds of the cytoplasm into the vacuole. Very small crescent bodies were observed in the parasitophorous vacuoles of several zygotes of E. nieschulzi between the vacuole membrane (mv) and the outermost parasite membrane (ml).

## Microgametocytes

As reported by other authors (11, 17, 46, 47), early microgametocytes were difficult to distinguish from early schizonts. Positive identification was considered to be the presence of centrioles between the plasmalemma and the nucleus, as reported for E. ferrisi (47). Centrioles were observed closely associated with the surface membranes and mitotic figures in mono- and multinucleate microgametocytes of E. nieschulzi, whereas centrioles did not appear until completion of nuclear divisions in E. auburnensis (20, 53) and E. falciformis (53). Two pairs of centrioles were seen between the surface membrane and some dividing nuclei of E. nieschulzi as reported in E. auburnensis (20, 53) and E. labbeana (68). The postdivision nucleus of E. nieschulzi had only a single pair of centrioles, as seen in all other Eimeria species (17, 46, 53). As well as in microgametocytes, centrioles were also present in schizonts during nuclear division, but were not associated with the surface membrane (9, 10, 18, 24, 26). An early macrogametocyte in the present study also had a centriole associated with a thickening of both membranes of the nuclear envelope. Centrioles have not been reported previously in macrogametocytes.

Nuclear divisions in E. nieschulzi, as in all other sporozoans (17, 46, 53), occur by eccentric intranuclear spindles termed 'centrocones' by Dubremetz (9). The centrocones of E. necatrix (9), E. callospermophili (18), E. magna (18, 61), and E. tenella (24) were situated within the perinuclear space and had spindle microtubules which passed through pores in the inner nuclear membrane and radiated inward into the nucleoplasm. In E. nieschulzi, some spindle microtubules terminated in kinetochores on loosely coiled chromosomes aggregated into a metaphase plate and others extended past the chromatin mass. Asters of microtubules were reported associated with mitotic figures in E. ninakohylakamovae (26) but were never seen in E. nieschulzi or any other coccidian species (17, 46, 53). The nuclear envelope in E. nieschulzi, as in all other sporozoans (17, 46, 53), remained intact during nuclear divisions.

The nucleolus was quite prominant in early nuclear divisions of E. nieschulzi, but was reduced with successive divisions and ultimately disappeared or was obscured by dense chromatin. Nucleoli were lacking entirely in microgametocytes of E. brunetti (11) and E. ferrisi (47).

Nuclear chromatin in E. nieschulzi microgametocytes was initially finely granular euchromatin, as in late trophozoites, and became more densely clumped and peripheral with successive divisions. The chromatin in E. brunetti (11), E. intestinalis (4, 5), E. ferrisi (47), and E. magna (5, 61) was clumped at the periphery of the nucleus even in early divisions. The overall size of the nucleus of E. nieschulzi was reduced by about 40% between the first nuclear division and the postdivision stage when chromatin was condensed at one side of the nucleus. Similar

reductions in nuclear size were reported in E. brunetti (11), E. intestinalis (5, 59), and E. magna (5, 59). The nuclear chromatin became segregated to the side of the nucleus closest to the plasmalemma and condensed to form crescent shaped masses in E. nieschulzi, as reported in all other coccidian species studied (17, 46, 53). After nuclear condensation, E. auburnensis underwent one further set of nuclear divisions (20, 53), apparently producing two microgametes from each nucleus, whereas E. nieschulzi and all other coccidian species studied (17, 46, 53) produced a single microgamete from each condensed nucleus. Only the condensed portion of the nucleoplasm was incorporated into the microgamete of E. nieschulzi, as reported in all other coccidian species studied except E. perforans (22, 53), in which the entire nucleus was reportedly included.

As the microgametocyte of E. nieschulzi developed, there was a great increase in endoplasmic reticulum and in the number of mitochondria. A few lipid bodies and numerous amylopectin bodies were formed in intermediate microgametocytes in close association with endoplasmic reticulum. Amylopectin inclusions were not seen in mature microgametocytes of E. acervulina (53) or E. brunetti (11), occurred in only 5% of E. labbeana microgametocytes, and were observed only after differentiation of microgametes in E. ferrisi (47).

In E. nieschulzi, deep invaginations of the single limiting membrane containing numerous micropores vastly increased the surface area, forming a so-called polycentric microgametocyte (46). Similar invaginations were also seen in E. auburnensis (20, 22), E. brunetti (11), E. labbeana (68), E. magna (5, 18, 61), and E. maxima (35). Scholtyseck et al. (47)

stated that only large microgametocytes which produced many microgametes were polycentric, but E. labbeana has the smallest mature microgametocyte yet described (68) and E. nieschulzi microgametocytes are smaller than those of E. bovis, E. intestinalis, E. pragensis, E. stiedai, and T. gondii, all of which are not invaginated and therefore monocentric (53).

Areas of electron dense inner membrane appeared between the surface membrane and the centriolar pair above each nucleus before chromatin condensation in E. nieschulzi. Similar structures in E. magna (61) and E. brunetti (11) were reported to be anlage of the perforatorium. Such inner membrane segments may also give rise to the dense ring which is involved in pinching off the complete microgamete. 'Dense rings', 'dense collars', or 'underlying cylinderlike osmiophilic layers' have been reported beneath the surface membrane of the stalk of microgametocytes during the process of gamete differentiation in most Eimeria species (5, 7, 11, 20, 22, 24, 35, 36, 47, 53, 59, 61). The point of attachment of the stalk was invariably just posterior to the basal bodies. In early studies of E. intestinalis (4, 5), E. nieschulzi (7), E. tenella (24), and T. gondii (53), the dense rings were mistaken for micropores. In the present study, two ring shaped microtubules were observed in the most constricted portion of the dense ring. The substructure of this organelle has not been reported previously.

The anteriormost tip of the microgamete of Eimeria species (53) contains a spire shaped electron dense structure termed 'perforatorium' by Cheissin (4). An electron dense plate or 'plaque' (11) extends for

some distance from the apex posteriorly just beneath the surface membrane. In T. gondii (17, 53), this posterior region of the perforatorium was reported to consist of 15-16 short microtubules, while in E. brunetti (11), it was described as membranous with short projections away from the surface. In E. nieschulzi, the perforatorium plate appeared as a membrane with bead-like electron dense structures on the inner surface and which extended posteriad to a point just anterior to the tip of the nucleus where it terminated in an electron dense bulbous structure not seen in other species.

During the nuclear condensation process in E. nieschulzi, the centrioles (basal bodies) shifted their orientation from perpendicular to the surface of the nucleus and parallel to each other, to parallel with the surface of the nucleus and perpendicular to each other. The basal bodies were connected by a highly electron dense rootlet composed of helical fibers. In other studies, this structure appeared as a dense homogeneous matrix common to microgametes of all Eimeria species (17, 46, 53) and which was described as a reinforcement for the perforatorium and a strong foundation for the attachment of flagella in E. brunetti (11). Ferguson et al. speculated that such connection between basal bodies might function in coordination of flagellar movement (11). In E. brunette (11), it was reported that the central tubule of the centriole disappeared upon transformation to a basal body and subsequent flagellar outgrowth. The proximal (closed) portion of the basal bodies in E. nieschulzi were nearly obscured by the flagellar rootlet, but a short central microtubule was visible in some sections.

Flagella are formed from the basal bodies by extension of micro-

tubules into outpocketings in the gametocyte plasmalemma (46). Microgametes of E. perforans (22, 53) and E. falciformis (53) were reported to posess three flagella; those of E. auburnensis (20, 53), E. maxima (36, 53), E. nieschulzi (7, 53), and E. tenella (24, 53) had two free flagella and a short third flagellum attached for most of its length. Microgametes of E. brunetti (11), E. ferrisi (47), E. intestinalis (5, 53, 59), E. labbeana (68), E. magna (5, 18, 53, 61), E. pragensis (53), T. gondii (53), and E. nieschulzi in the present study had only two free flagella. The more posteriorly arising flagellum in the latter group remained in contact with the body of the microgamete posteriad to about the anterior tip of the nucleus.

Longitudinal microtubules, which differ in number and position with species, in the body of microgametocytes have been described as a rudimentary flagellum in several species (47, 53, 61, 68). Ferguson et al. (11) expressed the opinion that body microtubules in microgametes of E. brunetti functioned in support of the nucleus and mitochondrion and did not constitute a rudimentary flagellum. Since body microtubules in E. nieschulzi are not extensions of a basal body as are active flagella, this author concurs with the support hypothesis.

# SUMMARY

Sexual development of Eimeria nieschulzi parallels development of other Eimeria species fairly closely, with certain exceptions. The major importance of this study is the characterization of the complete process of oocyst wall formation and the description of structures, both in micro- and macrogametocytes, that were not well visualized in previous studies.

The outer layer of the oocyst wall formed between membranes 2 and 3 (numbered from the most peripheral) from fine granular material produced by disintegration of type 1 wall forming bodies and partial disintegration of type 2 wall forming bodies. The material which formed the outer layer was transported across the limiting membrane, membrane 4, and membrane 3 which appeared in segments. Outer wall layers may or may not have coalesced before deposition of the inner wall layer. Material forming the inner wall layer came from further breakdown of type 2 wall forming bodies and from small electron dense bodies, and was exocytosed into a space between membranes 4 and 5. Membranes 6 and 7 were observed at the surface of the sporont before coalescence of the oocyst wall, which progressed from membrane complex 3-4 outward in the outer layer and inward in the inner layer.

The sporont contracted within the completed oocyst and formed a fluid filled space. Membranes 5, 6, and 7 remained at the surface of the sporont during contraction. Only small granular residua of wall forming bodies remained in the sporont cytoplasm after completion of the oocyst wall.

Microgametes of E. nieschulzi were biflagellate and contained a condensed nucleus, a single elongate mitochondrion, 3 longitudinal body microtubules, 2 basal bodies connected by a helical fibrous flagellar rootlet, and a dense granular perforatorium that terminated posteriorly in a bulbous electron dense structure. Microgametes were pinched-off from the surface of microgametocytes by a dense ring which, in this study, appeared to contain 2 ring-like microtubules. The substructure of the flagellar rootlet and the dense ring have not been reported previously in Eimeria.

# APPENDIX

Preliminary attempts to study ultrastructural changes during sporulation of Eimeria nieschulzi oocysts were not successful. To study fine structure within the formed oocyst wall it is necessary to either (i) mechanically disrupt the oocyst wall, (ii) chemically disrupt the wall, or (iii) partially degrade the wall by chemical means so as to increase the permeability and facilitate infiltration of fixatives and embedding resins without damaging or altering the cytoplasmic mass(es) within. It was possible to strip away the outer layer of the oocyst wall in 2.5% sodium hypochlorite (NaOCl) (43) but treatment of stripped oocysts with 2:1 chloroform-methanol, concentrated sulfuric acid, or proteolytic enzymes did not appear to alter the permeability of the inner wall layer. Epoxy embedments of pelleted oocysts subjected to the above chemical treatments and extended dehydration and infiltration regimes were very difficult to thin section with glass knives and contained only collapsed specimens when examined microscopically.

Mechanical disruption of the oocyst wall was attempted with (i) a Thomas tissue homogenizer and (ii) a Ribi cell fractionator. It was found that vigorous treatment of sporulated oocyst in the tissue homogenizer for 16 minutes ruptured about 75% of the oocysts and released sporocysts and free sporozoites. Similarly, sporulated oocysts subjected to 900 to 1,000 pounds per square inch in the Ribi press were nearly all ruptured, releasing sporozoites. Lesser pressures had little or no effect on oocyst walls.

Feces from infected animals were collected frequently and refrigerated in 2.5% $K_2Cr_2O_7$. Samples were pooled until the infection was passed and then the unsporulated oocysts were extracted and concentrated as outlined in the Materials and Methods before warming to room temperature to begin sporulation. Aliquots were withdrawn at 12 hour intervals and subjected to the above listed chemical treatments, the Ribi cell fractionator, or the Thomas tissue homogenizer. Samples for mechanical disruption were suspended in 3% glutaraldehyde in 0.2 molar cacodylate buffer at pH 7.2 for the treatment. After treatment, samples were dehydrated and infiltrated in suspension, then finally repelleted in Spurr's epoxy resin by high speed centrifugation of the embedding molds containing suspensions of oocyst fragments and epoxy resin. As noted with the chemically treated samples, epoxy embedments of mechanically fractured oocysts were extremely difficult to thin section with glass knives due to the hardness of the oocyst wall fragments. No intact cytoplasmic masses could be found in sections from those embedments, indicating that rupture of the sporont accompanied rupture of the oocyst wall under the conditions employed.

Birch-Andersen et al. (1) reported success in thin sectioning oocysts by a frozen section technique, although the fine detail obtained was less than that desired. Although a Christiansen frozen thin sectioning attachment for ultramicrotomy was available, use demands on the single ultramicrotome available at the University of Montana precluded employment of that technique.

# LITERATURE CITED


1. Birch-Andersen A, Ferguson DJP, Pontrefract RD. 1976. A Technique for Obtaining Thin Sections of Coccidian Oocysts. Acta. Path. Microbiol. Scand. Sect. B, 84, 235-9.

2. Cheissin EM. 1935. Structure de l'Oocyste et Permeabilite de ses Membranes chez les Coccidies du Lapin. Ann. Parasitol. 13, 133-64.

3. Cheissin EM. 1959. Cytochemical Investigations of Different Stages of the Life Cycle of Coccidia of the Rabbit. Proc. XVth Int. Zool. London 713-6.

4. Cheissin EM. 1964. Electron Microscope Study of Microgametocytes of Eimeria intestinalis (Sporozoa, Coccidia). Zool. Zh. 43:5 647-50. (in Russian, English translation by Library Branch NIH Bethesda, MD)

5. Cheissin EM. 1965. Electron Microscopic Study of Microgametogenesis in Two Species of Coccida from Rabbit (Eimeria magna and E. intestinalis). Acta. Protozool. Vol. III, 19 215-34.

6. Chobotar B, Senaud J, Ernst JV, Scholtyseck E. 1975. The Ultrastructure of Macrogametes of Eimeria ferrisi Levine and Ivens 1965 in Mus musculus. Z. Parasitenk. 48, 111-21.

7. Colley FC. 1967. Fine Structure of Microgametocytes and Macrogamonts of Eimeria neischulzi. J. Protozool. 14, 663-74.

8. Cross JB. 1947. A Cytologic Study of Toxoplasma with Special Reference to its Effect on the Host's Cell. J. Infect. Dis. 80, 278-96.

9. Dubremetz J-F. 1971. L'Ultrastructure du Centriole et du Centrocone chez la Coccidie Eimeria necatrix. Etude au Cours de la Schizogonie. J. Microscopie 12, 453-8. (in French)

10. Dubremetz J-F. 1973. Etude Ultrastructurale de la Mitose Schizogonique chez la Coccidie Eimeria necatrix (Johnson 1930). J. Ultrastruct. Res. 42, 354-76. (in French, English summary)

11. Ferguson DJP, Birch-Andersen A, Hutchison WM, Siim JC. 1977. Ultrastructural Studies on the Endogenous Development of Eimeria brunetti. II. Microgametogony and the Microgamete. Acta. Path. Microbiol. Scand. Sect. B, 85, 67-77.

12. Ferguson DJP, Birch-Andersen A, Hutchison WM, Siim JC. 1977. Ultrastructural Studies on the Endogenous Development of Eimeria brunetti. III. Macrogametogony and the Macrogamete. Acta. Path. Microbiol. Scand. Sect. B, 84, 78-88.

13. Ferguson DJP, Birch-Andersen A, Hutchison WM, Siim JC. 1977. Observations on the Ultrastructure of the Late Sporoblast and Initiation of Sporozoite Formation in Eimeria brunetti. Acta. Path. Microbiol. Scand. Sect. B, 85, 110-12.

14. Gill BS, Ray NH. 1954. Glycogen and its Probable Significance in Eimeria tenalla. Railliet and Lucet, 1891. Ind. J. Vet. Sci. 24, 223-8.

15. Grasse PP. 1953. Traite de Zoologie, Vol. 1 Pt. 2 Masson, Paris.

16. Hammond DM. 1973. Life Cycles and Development of Coccidia. in Hammond DM, Long PL, eds., The Coccidia, University Park Press, Baltimore. 46-79.

17. Hammond DM. 1973. Ultrastructure and Development of Coccidia. in Proceedings of the Symposium on Coccidia and Related Organisms. University of Guelph, Guelph, Ontario. 11-44.

18. Hammond DM, Roberts WL, Youssef NN, Danforth HD. 1973. Fine Structure of the Intranuclear Spindle Poles in Eimeria callospermophili and E. magna. J. Parasit. 59, 581-4.

19. Hammond DM, Scholtyseck E. 1970. Observations Concerning the Process of Fertilization in Eimeria bovis. die Naturwissenschaften 57, 399.

20. Hammond DM, Scholtyseck E, Chobotar B. 1969. Fine Structural Study of Microgametogenesis of Eimeria auburnensis. Z. Parasitenk. 33, 65-84.

21. Hammond DM, Scholtyseck E, Chobotar B. 1967. Fine Structures Associated with Nutrition of the Intracellular Parasite Eimeria auburnensis. J. Protozool. 14, 678-83.

22. Hammond DM, Scholtyseck E, Miner ML. 1967. Fine Structure of Microgametocytes of Eimeria perforans, E. stiedae, E. bovis, and E. auburnensis. J. Parasit. 59, 1071-9.

23. Henry DP. 1932. The Oocyst Wall in the Genus Eimeria. Univ. Calif. Publ. Zool. 37, 269-79.

24. Hoppe G. 1976. The Ultrastructure of Early Generation Development and Later Schizonts of Eimeria tenella in the Chicken. Protistologica 12, 169-81.

25. Kelley GL, Hammond DM. 1972. Fine Structural Aspects of Early Development of Eimeria ninakohlyakimovae in Cultured Cells. Z. Parasitenk. 38, 271-84.

26. Kelley GL, Hammond DM. 1973. Fine Structural Aspects of Nuclear Division and Merogony of Eimeria ninakohlyakimovae in Cultured Cells. J. Parasit. 59, 1071-9.

27. Lee DL, Millard BJ. 1971. The Structure and Development of the Macrogamete and Oocyst of Eimeria acervulina. Parasitology 62, 31-4.

28. Lee E-H, Remmler O, Fernando MA. 1977. Sexual Differentiation in Eimeria tenella (Sporozoa:Coccidia). J. Parasit. 63, 155-6.

29. Levine ND. 1962. Protozoan Parasites of Domestic Animals and Man. Brugess Publishing Co., Minneapolis. 158-253.

30. Levine ND. 1962. Protozoology Today. J. Protozool. 9, 1-6.

31. Levine ND. 1973. Introduction, History, and Taxonomy. in Hammond DM, Long PL, eds., The Coccidia, University Park Press, Baltimore. 1-22.

32. Levine ND. 1973. Historical Aspects of Research on Coccidiosis. in Proceedings of the Symposium on Coccidia and Related Organisms. University of Guelph, Guelph, Ontario. 1-10.

33. Marquardt WC. 1966. The Living Endogenous Stages of the Rat Coccidium Eimeria nieschulzi. J. Protozool. 13, 509-14.

34. McDougald LR, Jeffers TK. 1976. Eimeria tenella (Sporozoa, Coccidia): Gametogony Following a Single Asexual Generation. Science 192, 258-9.

35. Mehlhorn H. 1972. Elektronenmikroskopische Untersuchungen an Entwicklungsstadien von Eimeria maxima (Sporozoa Coccidia). II. Die Feinstruktur der Microgameten. Z. Parasitenk. 40, 151-63.

36. Mehlhorn H. 1972. Elektronenmikroskopische Untersuchungen an Entwicklungsstadien von Eimeria maxima aus dem Hauscuhn. III. Der Differenzierungsprozess der Mikrogameten unter besonderer Berucksichtigung der Kernteilungen. Z. Parasitenk. 40, 243-60.

37. Michael E. 1975. Structure and Mode of Function of the Organelles Associated with Nutrition of the Macrogametes of Eimeria acervulina. Z. Parasitenk. 45, 347-61.

38. Monne L, Honig G. 1954. On the Properties of the shells of the Coccidian Oocysts. Ark Zool., Stockholm. 7, 251-6.

39. Odense PH, Logan VH. 1976. Prevalence and Morphology of Eimeria gadi (Fiebiger 1913) in the Haddock. J. Protozool. 23, 564-71.

40. Pattillo WH, Becker ER. 1955. Cytochemistry of Eimeria brunetti and E. acervulina of the Chicken. J. Morphol. 96, 61-95.

41. Pellérdy LP. 1974. Coccidia and Coccidiosis. 2nd edition. Verlag Paul Parey, Berlin. 584-7.

42. Roberts WL, Speer CA, Hammond DM. 1970. Electron and Light Microscope Studies of the Oocyst Walls, Sporocysts, and Excysting Sporozoites of Eimeria callospermophili and E. larimerensis. J. Parasitol. 56, 918-26.

43. Ryley JF. 1973. Cytochemistry, Physiology, and Biochemistry, in Hammond DM, Long PL, eds., The Coccidia, University Park Press, Baltimore. 145-82.

44. Ryley JF, Bently M, Manners DJ, Stark JR. 1969. Amylopectin, the Storage Polysaccharide of the Coccidia Eimeria brunetti and E. tenella. J. Parasitol. 55, 839-45.

45. Scholtyseck E. 1962. Electron Microscope Studies on Eimeria perforans (Sporozoa). J. Protozool. 9, 407-14.

46. Scholtyseck E. 1973. Ultrastructure. in Hammond DM, Long PL, eds., The Coccidia, University Park Press, Baltimore. 81-144.

47. Scholtyseck E, Chobotar B, Senaud J, Ernst JV. 1977. Fine Structure of Microgametogenesis of Eimeria ferrisi Levine and Ivens 1965 in Mus musculus. Z. Parasitenk. 51, 229-40.

48. Scholtyseck E, Gonnert R, Haberkorn A. 1969. Die Feinstruktur der Makrogameten des Huhnercoccids Eimeria tenella. Z. Parasitenk. 33, 31-43. (in German, English summary)

49. Scholtyseck E, Hammond DM. 1970. Electron Microscope Studies of Macrogametes and Fertilization in Eimeria bovis. Z. Parasitenk. 34, 310-8.

50. Scholtyseck E, Hammond DM, Ernst JV. 1966. Fine Structure of the Macrogametes of Eimeria perforans, E. stiedae, E. bovis, and E. auburnensis. J. Parasit. 52, 975-87.

51. Scholtyseck E, Mehlhorn H, Haberkorn A. 1971. Die Feinstrukture der Makrogameten des Mausecoccids Eimeria falciformis. Z. Parasitenk. 37, 44-54. (in German, English summary)

52. Scholtyseck E, Mehlhorn H, Hammond DM. 1971. Fine Structure of Macrogametes and Oocysts of Coccidia and Related Organisms. Z. Parasitenk. 37, 1-43.

53. Scholtyseck E, Mehlhorn H, Hammond DM. 1972. Electron Microscope Studies of Microgametogenesis in Coccidia and Related Groups. Z. Parasitenk. 38, 95-131.

54. Scholtyseck E, Voigt W-H. 1964. Die Bildung der Oocystenhulle bei Eimeria perforans (Sporozoa). Z. Zellforsch. 62, 279-92. (in German)

55. Scholtyseck E, Volkmann B, Hammond DM. 1966. Spezifische feinstrukturen bei Parasit und Wirt als Ausdruck ihrer Wechselwirkungen am Beispiel von Coccidien. Z. Parasitenk. 28, 78-94. (in German)

56. Seliverstova VG. 1969. Some Data on the Ultrastructure of Macrogametes of Eimeria tenella (Sporozoa, Coccidia). Acta. Protozool. 12, 49-61. (in Russian, English summary, English translation by Language Service Bureau)

57. Seliverstova VG. 1970. (Some Data on the Oocyst Sheath Formation in Eimeria tenella) Tsitologiya 12, 238-42. (in Russian)

58. Shirley MW, Millard BJ. 1976. Some Observation on the Sexual Differentiation of Eimeria tenella using Single Sporozoite Infection in Chicken Embryos. Parasitology 73, 337-41.

59. Snigirevskaya YS. 1969. Changes in Some Ultrastructures during Microgametogenesis in Rabbit Coccidia. Tsitologiya (Cytology) 11, 382-5. (in Russian, English summary, English translation by Language Service Bureau)

60. Snigirevskaya YS. 1969. Electron Microscopic Study of Eimeria intestinalis Macrogametes. Tsitologiya (Cytology) 11, 700-6. (in Russian, English summary, English translation by Language Service Bureau)

61. Speer CA, Danforth HD. 1976. Fine Structural Aspects of Microgametogenesis of Eimeria magna in Rabbits and in Kidney Cell Cultures. J. Protozool. 23, 109-15.

62. Speer CA, Duszynski DW. 1975. Fine Structure of the Oocyst Walls of Isospora serini and Isospora canaria and Excystation of Isopora serini from the Canary, Serinus canarius L. J. Protozool. 22, 476-81.

63. Speer CA, Hammond DM. 1972. Development of Gametocytes and Oocysts of Eimeria magna from Rabbits in Cell Culture. Proc. Helminth. Soc. Wash. 39, 114-8.

64. Speer CA, Hammond DM, Youssef NN, Danforth HD. 1973. Fine Structural Aspects of Macrogametogenesis in Eimeria magna. J. Protozool. 20, 274-81.

65. Thiery JP. 1967. Mise en Evidence des Polysaccharides sur Coupes Fines en Microscopie Electronique. J. Microscopie 6, 987-1018. (in French)

66. Varghese T. 1975. The Fine Structure of Endogenous Stages of Eimeria labbeana: 2. Mature Macrogamonts and Young Oocysts. Z. Parasitenk. 46, 43-51.

67. Varghese T. 1976. Fine Structure of the Endogenous Stages of Eimeria labbeana: 3. Feeding Organelles. Z. Parasitenk. 49, 25-32.

68. Varghese T. 1976. The Fine Structure of Endogenous Stages of Eimeria labbeana: 4. Microgametogenesis. Z. Parasitenk. 50, 227-35.

69. Wagenbach GE, Challey JR, Burns WC. 1966. A Method for Purifying Oocysts Employing Clorox and Sulfuric Acid Dichromate Solution. J. Parasit. 52, 1222.

70. Wheat BE, Jensen JB, Ernst JV, Chobotar B. 1976. Ultrastructure of Macrogametogenesis of Eimeria mivati. Z. Parasitenk. 50, 125-36.

71. Wilson PAG, Fairbairn D. 1961. Biochemistry of Sporulation in Oocysts of Eimeria acervulina. J. Protozool. 8, 410-16.

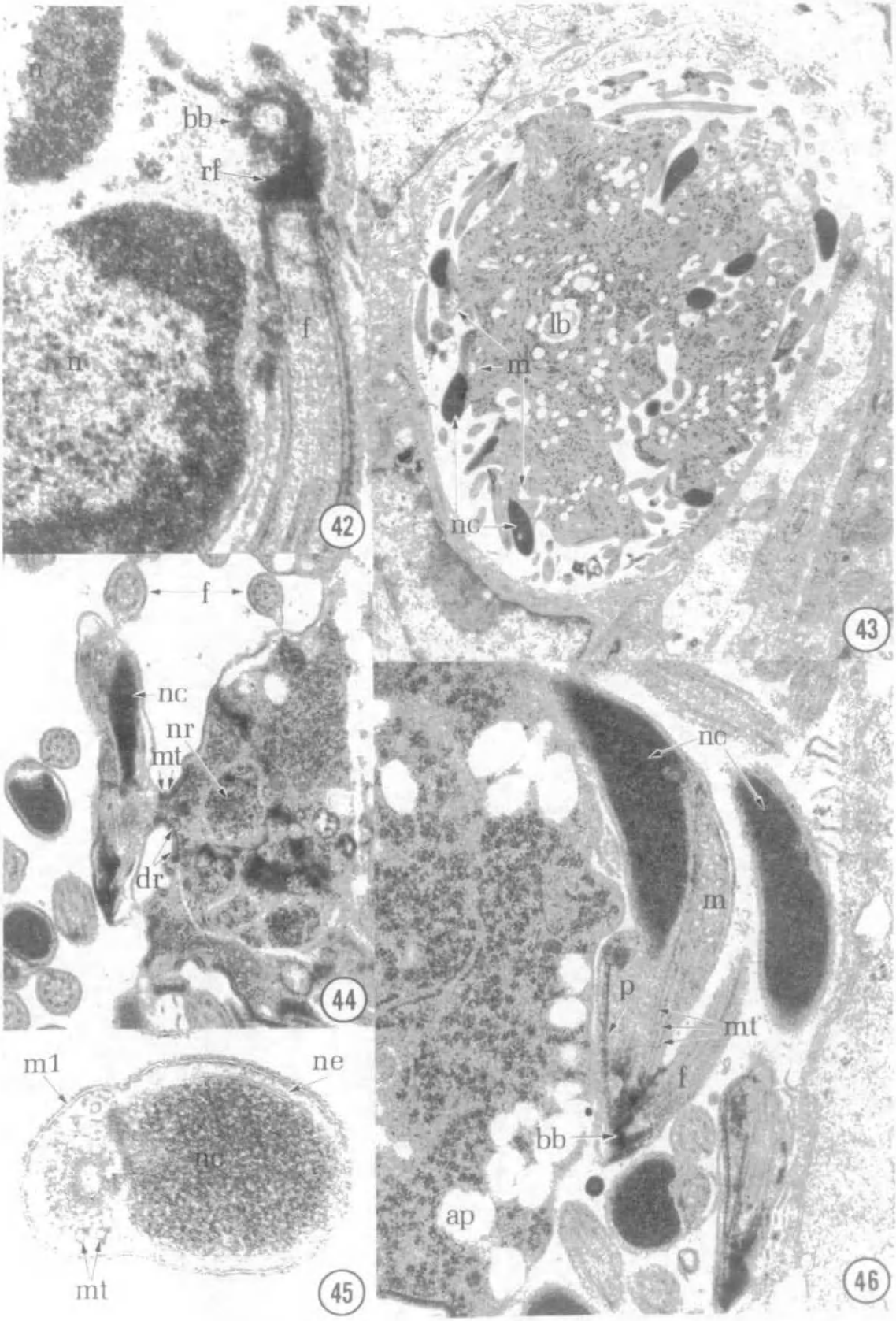
n
bb
rf
f
n
42
lb
m
nc
43
f
nc
nr
mt
dr
44
nc
m
p
mt
f
bb
ap
46
m1
ne
nc
mt
45